UCONN LIBRARY

University of Connecticut
OpenCommons@UConn

UCHC Articles - Research

University of Connecticut Health Center Research

1-2013

Neurogenesis Continues in the Third Trimester of Pregnancy and Is Suppressed by Premature Birth

Nada Zecevic
University of Connecticut School of Medicine and Dentistry

Follow this and additional works at: https://opencommons.uconn.edu/uchcres_articles

 Part of the Medicine and Health Sciences Commons

Recommended Citation
Zecevic, Nada, "Neurogenesis Continues in the Third Trimester of Pregnancy and Is Suppressed by Premature Birth" (2013). *UCHC Articles - Research*. 198.
https://opencommons.uconn.edu/uchcres_articles/198

NIH Public Access
Author Manuscript
J Neurosci. Author manuscript; available in PMC 2013 July 15.

Published in final edited form as:
J Neurosci. 2013 January 9; 33(2): 411–423. doi:10.1523/JNEUROSCI.4445-12.2013.

Neurogenesis Continues in the Third Trimester of Pregnancy and Is Suppressed by Premature Birth

Sabrina Malik, MD[1], **Govindaiah Vinukonda, PhD**[1], **Linnea R. Vose, PhD**[1], **Daniel Diamond, BS**[1], **Bala B.R. Bhimavarapu, MD**[2], **Furong Hu, BA**[1], **Muhammad T. Zia, MD**[1], **Robert Hevner, MD, PhD**[3], **Nada Zecevic, MD, PhD**[4], and **Praveen Ballabh, MD**[1,2]

[1]Department of Pediatrics, New York Medical College-Westchester Medical Center, Valhalla, NY

[2]Cell Biology and Anatomy, New York Medical College-Westchester Medical Center, Valhalla, NY

[3]Department of Neurological Surgery, University of Washington, Seattle, Washington

[4]Department of Neuroscience, University of Connecticut Health Center, Farmington, CT

Abstract

Premature infants exhibit neurodevelopmental delay and reduced growth of the cerebral cortex. However, the underlying mechanisms have remained elusive. Therefore, we hypothesized that neurogenesis in the ventricular and subventricular zones of the cerebral cortex would continue in the third trimester of pregnancy, and that preterm birth would suppress neurogenesis. To test our hypotheses, we evaluated autopsy materials from human fetuses and preterm infants of 16–35 gestational weeks (gw). We noted that both cycling and non-cycling $Sox2^+$ radial glial cells as well as $Tbr2^+$ intermediate progenitors were abundant in human preterm infants until 28 gw. However, their densities consistently decreased from 16 through 28 gw. To determine the effect of premature birth on neurogenesis, we employed a rabbit model and compared preterm (E29, 3 days old) and term pups (E32, <2h age) at an equivalent post-conceptional age. Glutamatergic neurogenesis was suppressed in preterm rabbits, as indicated by reduced number of $Tbr2^+$ intermediate progenitors and increased number of $Sox2^+$ radial glia. Additionally, hypoxia inducible factor-1α, vascular endothelial growth factor, and erythropoietin were higher in term than preterm pups, reflecting the hypoxic intrauterine environment of just-born term pups. Proneural genes, including Pax6, Neurogenin-1 and -2, were higher in preterm rabbit pups compared to term pups. Importantly, neurogenesis and associated factors were restored in preterm pups by treatment with dimethyloxallyl glycine—a hypoxia mimetic agent. Hence, glutamatergic neurogenesis continues in the premature infants, preterm birth suppresses neurogenesis, and hypoxia-mimetic agents might restore neurogenesis, enhance cortical growth, and improve neurodevelopmental outcome of premature infants.

Keywords

Neurogenesis; radial glia; intermediate progenitors; Tbr2; preterm infant; Hypoxia

Introduction

The human cerebral cortex is complex and highly organized, which distinguishes humans from other species. The cerebral cortex orchestrates cognitive functions, intelligence, motor

Address for Correspondence: Praveen Ballabh, MD, Regional Neonatal Center, Maria Fareri Children's Hospital at Westchester Medical Center., Valhalla, NY 10595, Phone: 914-493-8558 Fax: 914-493-1005, Pballabh@msn.com.

NIH-PA Author Manuscript
NIH-PA Author Manuscript
NIH-PA Author Manuscript

NIH-PA Author Manuscript

NIH-PA Author Manuscript

NIH-PA Author Manuscript

abilities, and sensory perceptions. Unraveling its development after mid-pregnancy might elucidate the mechanisms of its expansion and enhance the understanding of neurological disorders in premature infants. Therefore, we asked whether neurogenesis continues in prematurely born infants.

Every year, about 15 million infants are born preterm worldwide. These infants exhibit significant reduction in cortical gray matter volume and manifest with moderate-to-severe neurodevelopmental disability at 1 year of age (Dyet et al., 2006; Thompson et al., 2007). They continue to display impaired cortical growth even in childhood and adolescence (de Kieviet et al., 2012). Premature infants frequently develop complications, including intraventricular hemorrhage, hypoxia, ischemia, and sepsis, which reduce cortical growth and development (Vasileiadis et al., 2004). These neonatal disorders may impact neurogenesis, causing an imbalance between excitatory glutamatergic and inhibitory GABAergic neurons. The imbalance of excitation and inhibition within neural microcircuitry is associated with epilepsy, autism, neurodevelopmental disorders, and psychiatric illnesses, which are more common in preterm than term infants (Whitaker et al., 1997; Indredavik et al., 2010). Hence, it is important to determine how developmental neurogenesis progresses during the third trimester of pregnancy when premature infants are born.

In primates, glutamatergic neurogenesis occurs in the ventricular (VZ) and subventricular zones (SVZ) of the dorsal telencephalon, whereas GABAergic neurogenesis takes place in both ventral (ganglionic eminence) and dorsal telencephalon (Letinic et al., 2002; Jakovcevski et al.). Cortical projection neurons, which are primarily glutamatergic, originate from radial glia residing in the dorsal VZ and SVZ. Radial glial cells in the VZ generate intermediate progenitor cells (IPC) that migrate to the SVZ to further divide, migrate, and form the six cortical layers (Haubensak et al., 2004). During infancy, migrating immature neurons have been found to be abundant in the SVZ and rostral migratory system of (Sanai et al., 2011). Neurogenesis has been studied in less than 24 gw and in term infants (Hansen et al., 2010; Wang et al., 2011), but not in preterm infants (24–35 gw).

Neurogenesis is temporally regulated, and premature birth might affect it. Oxygen is a key regulator of neurogenesis (Panchision, 2009). Oxygen concentration in cerebral circulation is 25–30 mm Hg in fetuses (*in utero*), which increases to 50–60 mm Hg shortly after premature birth (Soothill et al., 1986). Increasing evidence indicates that hypoxia enhances proliferation of neuronal progenitors *in vitro* (Horie et al., 2004). Thus, a withdrawal of physiological hypoxia with premature birth might suppress neuronal differentiation (Horie et al., 2008). Hypoxia activates hypoxia-inducible factor (HIF)-1α, which regulate erythropoietin (EPO), vascular endothelial growth factor (VEGF), WNT/β-catenin activity, and several signaling pathways (Zheng et al., 2008). These factors exert direct effects on neurogenesis. Therefore, we hypothesized that neurogenesis in the VZ and SVZ of the cerebral cortex would continue in the third trimester of pregnancy and that preterm birth might suppress neurogenesis. We also postulated that the HIF-1α activation would restore neurogenesis in premature infants.

Material and Methods

Human subjects

The Institutional Review Board at New York Medical College and Westchester Medical Center, Valhalla, NY approved the use of autopsy materials from fetuses and premature infants for this study. The study materials included brain tissues sampled from spontaneous abortuses of 16–22 gw and autopsies of premature infants of 23–40 gw. The autopsy samples were obtained at postmortem-interval of less than 18 h for premature infants and

NIH-PA Author Manuscript

NIH-PA Author Manuscript

NIH-PA Author Manuscript

less than 8 h for fetuses. Only infants of less than 5 d postnatal age were included in the study to minimize the effect of postnatal events on neurogenesis occurring in the neonatal intensive care units. We excluded premature infants with grade 2–4 intraventricular hemorrhage, major congenital anomalies, chromosomal defects, culture-proven sepsis, meningitis, hypoxic-ischemic encephalopathy, and infants receiving extracorporeal membrane oxygenator treatment from the study. Any brain tissue showing autolysis or necrosis on hematoxylin and eosin staining was also excluded. Autopsy samples were classified into 5 groups: a) fetuses of 16–19 gw, (n=5), b) fetuses of 20–22 gw (n=5), c) premature infants of 23–25 gw (n=5), d) premature infants of 26–28 gw (n=5), and e) premature infants of 29–35 gw (n=5). Of these, 10 were females and 15 were males. These samples were collected over the last 10 years (2002–2012) at New York Medical College-Westchester Medical Center, Valhalla, NY.

Human tissue collection and processing

Brain samples were processed as described previously (Ballabh et al., 2007). Coronal blocks (5–6 mm) were cut through frontal cortex (cortical plate), white matter (embryonic intermediate layer), and germinal matrix in the region of the thalamostriate groove at the level of interventricular foramen (Monro's foramen). The samples were fixed in 4% paraformaldehyde in phosphate buffer saline (PBS; 0.01 M, pH 7.4) for 18 h, cryoprotected by immersing into 20% sucrose in PBS buffer for 24 hours, followed by 30% sucrose for the next 24 h. We froze tissues after embedding them into optimum cutting temperature compound (Sakura, Japan); and then blocks were stored at −80°C. Frozen coronal blocks were cut into 12 μm sections using a cryostat and saved at −80°C until use.

Animal Experiments

The Institutional Animal Care and Use Committee of New York Medical College approved the use of animals for the study. We obtained timed-pregnant New Zealand rabbits from Charles River Laboratories, Inc. (Wilmington, MA). C-section was performed to deliver the pups prematurely at E29 (full-term=32 days). We kept the pups in an infant incubator pre-warmed to a temperature of 35°C. The pups were fed 2–3 ml (100 ml/kg) of puppy formula (Esbilac, Petag, IL) twice daily in the first two days; and subsequently, the feed was advanced to 125, 150, 200, 250 and 280 ml/kg at postnatal days 3, 5, 7, 10 and 14, respectively. We also included full-term (E32) rabbit pups in the study delivered by 2 pregnant rabbits. Live born and healthy looking pups were of either sex were included in the study. Pups with postnatal complications including aspiration of formula, cardiac arrest requiring resuscitation and any apparent congenital defect were excluded from the study.

Dimethyloxallyl glycine (DMOG) treatment

To stabilize HIF-1α, we treated E29 rabbit pups with DMOG (Caymen Chemicals, MI) starting immediately at birth. DMOG was administered in a dose of 100 mg/kg daily IM for 3 days. These pups were sacrificed at 72 h age. The comparison group received vehicle (15 μl DMSO).

Rabbit tissue collection and processing

We processed the tissues as previously described (Dummula et al., 2011). Two-to-three mm thick coronal slices, taken at the level of midseptal nucleus of the forebrain, were immersion-fixed in 4% paraformaldehyde in phosphate buffered saline (PBS; 0.01 M, pH 7.4) for 18 hours. Samples were then cryoprotected by immersing into 20% sucrose in 0.01 M PBS for 24 hours followed by 30% sucrose for the next 24 hours. Tissues were frozen into optimum cutting temperature compound. Frozen coronal blocks were cut on a cryostat into 30 μm sections.

NIH-PA Author Manuscript

NIH-PA Author Manuscript

NIH-PA Author Manuscript

Immunohistochemistry

Immunostaining was performed as described previously (Ballabh et al., 2007). The primary antibodies used in experiments included goat polyclonal SOX-2 (catalog # SC-6895, Santa Cruz Biotech, Santa Cruz, CA), rabbit polyclonal TBR2 (courtesy of Dr. Robert Hevner, Seattle, WA), rabbit monoclonal Ki67 (catalog # 275R-14, Cell Marque, Rocklin, CA), mouse monoclonal Ki67 (catalog # M7240, Dako, USA), mouse monoclonal phospho-vimentin (catalog # D076-3, MBL international, Woburn, MA), mouse monoclonal GFAP (catalog # G3893, Sigma, St. Louis, MO), and mouse monoclonal vimentin (catalog # V6630, Sigma, St. Louis, MO). The secondary antibodies used were Alexa 488 donkey anti-mouse, Alexa 647 donkey anti-goat, Alexa 594 donkey anti-rabbit (Invitrogen, Grand Island, NY). Briefly, we hydrated the fixed sections in 0.01 M PBS and incubated them with the primary antibodies diluted in PBS at 4°C overnight. After washing in PBS, the sections were incubated with secondary antibody diluted in 1% normal donkey serum in PBS at room temperature for 60 minutes. Finally, after washes in PBS, sections were mounted with Slow Fade Light Antifade reagent (Molecular Probes, Invitrogen, CA) and were visualized under a confocal microscope (Nikon Instruments, Japan). Stereology was performed using a Fluorescent microscope (Axioskop 2 plus, Carl Zeiss Inc.) with motorized specimen stage for automated sampling (ASI, Eugene, OR), CCD color video camera (Microfire, Optronics, Goleta, CA) and stereology software (Stereologer, SRC, Baltimore, MD).

Quantification of neuronal progenitors under confocal microscope

We quantified Sox2 and Tbr2 positive cells and their proliferation in 5 groups of subjects: 16–19, 20–22, 23–25, 26–28 and 29–35 gw (n = 5 each group, 25 subjects total). From each brain, 4–6 coronal sections were obtained. Coronal brain sections were triple labeled with Sox2, Tbr2 and Ki67 specific antibodies to evaluate density and proliferation of $Sox2^+$ and $Tbr2^+$ cells. To determine the proportion of $Sox2^+$ and $Tbr2^+$ cells compared to all neural cells, we labeled another set of coronal sections with Sox2, Tbr2 and Sytox (nuclear stain). The counting was done in six representative images from each brain region (dorsal cortical SVZ and ganglionic eminence) acquired on confocal microscope (Nikon Instruments, Japan) using 60 × objective. Of these, 3 images were taken at the level of the ventricular surface encompassing VZ and inner SVZ, and the remaining 3 images were acquired above the initial ones (outer SVZ). All counting was done on the confocal microscope (EZ-C1 program) by using ‘point of interest’ icon from menu bar. Hence, we counted objects in ~6 images per brain region (ganglionic eminence and dorsal SVZ) of each brain section (6 images × 2 brain regions × 4–6 sections × 25 brains). Stereological protocol was not followed for the quantification of cells in human brains because triple-labeled live images cannot be obtained by a regular fluorescent microscope equipped with stereology software. Hence, the counting was done on confocal microscope by an investigator blinded to the experimental group.

We also quantified doublecortin (DCX) labeled cells in four groups of human subjects: 16–22, 23–25, 26–28 and 29–35 gw (n = 4 each group, 16 subjects total). To this end, we triple labeled forebrain coronal sections with DCX, Ki67 and Sytox. The counting was done in dorsal cortical SVZ and ganglionic eminence, just as for Sox2 and Tbr2 by a blinded investigator on the confocal microscope.

Stereological assessment of Sox2, Tbr2 and Ki67 positive cells in rabbits

Unbiased stereology methods, with assistance from a computerized software system (*Stereologer*, Stereology Resource Center, Chester, MD), were used to quantify a range of parameters in two brain regions; a) dorsal VZ and SVZ underneath the corona radiata and corpus callosum and b) lateral ganglionic eminence (forms the lateral margin of the cerebral ventricles). Briefly, coronal sections were cut on cryostat at a setting of 30 μm thickness

NIH-PA Author Manuscript

NIH-PA Author Manuscript

NIH-PA Author Manuscript

with a section sampling interval of three (90μm) to achieve at least 6 sections at the level of mid-septal nucleus. The sections were triple-labeled with Sox2 or Tbr2 with Ki67 antibodies and DAPI (nuclear stain) and quantified as follows. The reference spaces (dorsal VZ and SVZ) were first outlined on the section under 5x objective. The volume of the outlined area (reference space) was quantified using a point counting probe (frame 25μm × 25μm; guard zone 2 μm; inter-frame interval = 300 μm). The total number of $Sox2^+$, $Tbr2^+$ or $Ki67^+$ cells labeled with their respective antibodies through a defined reference space was quantified using the optical dissector probe under 60x oil lens. For the optical dissector probe (frame 25 μm × 25 μm; guard zone 1 μm, interframe interval 200 μm), the user clicked on the objects within the dissector frame. Sampling continued until the coefficient of error (CE) was less than 0.10. To assess cells positive for both Ki67 and Sox2, we used a dual color filter (Filter set 74 HE GFP+mRFP shift free, Zeiss, Thornwood, NY) that visualizes both Alexa 488 and Alexa 594 labeled cells.

Western blot analyses

We homogenized the frozen brain tissue in sample buffer (3% SDS, 10% glycerol, 62.5mMol Tris-HCl, and 100 MM-MDTT) using a mechanical homogenizer and boiled the samples immediately for 5 minutes. The protein concentration in the supernatant was determined using BCA Protein Assay Kit (Pierce catalog # 23227, Thermo Scientifics, IL). Total protein samples were separated by SDS-PAGE according to the previously described method (Ballabh et al., 2007). Equal amounts of protein (10–20 μg) were loaded into a 4–15% gradient precast gel (Biorad, CA). The separated proteins were transferred onto polyvinylidene difluoride (PVDF) membrane by electro-transfer. The membranes were then incubated with primary antibodies (mouse monoclonal HIF-1α, catalog # SC-53546, Santa Cruz Biotech; mouse monoclonal VEGF catalog # SC-7269, Santa Cuz Biotech; rabbit polyclonal Pax6 catalog # PRB-278P, Covance, CA) . We detected target proteins with chemiluminescence ECL system (Amersham Biosciences Inc. NJ) by using secondary antibodies conjugated with horseradish peroxidase (Jackson Immunoresearch, PA). We next stripped the blots with stripping buffer (Pierce) and incubated with β actin primary antibody followed by secondary antibody and detection with chemiluminescence ECL system. As described previously (Ballabh et al., 2007), the blots from each experiment were densitometrically analyzed using ImageJ. The optical density values were normalized by taking the ratio of the target protein and β actin.

Quantitative real-time polymerase chain reaction

Quantitative real-time polymerase chain reaction (qRT-PCR) was performed as described previously (Ballabh et al., 2007). Briefly, total RNA were isolated from 1–2 mm thick slice taken at the level of mid-septal nucleus of the forebrain by Mini RNA isolation kit (Zymo Research, CA). RNA was reverse-transcribed using Superscript II RT (Invitrogen, CA). Real-time reverse transcriptase-PCR were used to analyze mRNA expression using an ABI PRISM 7700 Sequence Detection System (Applied Biosystems, USA). Quantification was performed using the efficiency-corrected ΔΔCT method. The following primers were used for qRT-PCR: Pax6 (accession # NM_001082217.1) sense CCCGTCCATCTTTGCTTGGGAAAT, antisense TAGCCAGGTTGCGAAGAACTCTGT; Neurogenin2 (accession # XM_002717014.1) sense GCATCAAGAAGACACGCAGACTGA, antisense TCTCGATCTTGGTTAGCTTGGCGT; Neurogenin 1 (accession # XM_002710221.1) sense AACCGCATGCACAACCTGAA, antisense AAGCGTAGCGTCTCGATCTT; Hes1 (accession # XM_002716517.1) sense GAGCACAGGAAGTCTTCAAAGCCA, antisense TGGAATGCCGCGAGCTATCTTTCT; Hes 5 (accession # NM_001010926.3) sense GCATCAACAGCAGCATCGAGCA, antisense TAGCTGACAGCCATCTCCAGGAT; Emx 1 (accession # BC037242.1) sense TCCAGAACCGGAGGACAAAGTACA, antisense

NIH-PA Author Manuscript

NIH-PA Author Manuscript

NIH-PA Author Manuscript

TGATGTGATGGGAGCCCTTCTTCT; Emx2 (accession # AF301598.1) sense AAGCGCTGCTTCACCATCGAGT, antisense AGCCGTTGAGGAACGGATTTATGG; Insulinoma associated 1 (Insm1; accession # NM_002196.2) sense ACTTCGAGGACGAGGTGACCA, antisense TTGCACAGCTGGCAGATGAACT; VEGF (accession # NM_003376)AGACGGACAGAAAGACAG (sense), AAGCAGGTGAGAGTAAGC (antisense).

Statistics and Analysis

Data are expressed as means ± standard error of the mean (sem). To determine differences in the density of radial glia, IP cells and their proliferation in the dorsal SVZ and ganglionic eminence in 5 age groups of human subjects, including 16–19, 20–22, 23–25, 26–28 and 29–35 gw, 2-way analysis of variance with repeated measures was used. The repeated factor was applied to the 2 brain regions, dorsal SVZ and ganglionic eminence. To compare the density of radial glia, IPC and their proliferation in treated preterm, untreated preterm and term rabbit pups, we used one-way ANOVA. For Western blot analyses, 3 group comparisons were done using one-way ANOVA. All post hoc comparisons to test for differences between means were done using Tukey multiple comparison test at the 0.05 significance level. For two group comparisons, either T-test or Mann Whitney U test was performed, as applicable.

Results

Radial glia and intermediate progenitors populate dorsal SVZ of premature infants

To evaluate neurogenesis, radial glia (apical progenitors) and IPC (basal progenitors) were assessed in the dorsal SVZ and VZ of five subgroups of human fetuses and premature infants: 16–19, 20–22, 23–25, 26–28 and 29–35 gw (n = 5 in each group, Table 1). We identified radial glia and IPC by immuno-labeling with antibodies for Sox2 and Tbr2 (T-brain gene 2) transcription factors, respectively. Ki67, which labels cells in late G1, S, G2, and M phases of the cell cycle, was chosen to assess proliferation of radial glia and IPC. Immunostaining of coronal sections revealed that $Sox2^+$ cells were abundant in the VZ and SVZ of fetuses and premature infants (Fig. 1 and 2). However, their densities decreased with advancing gestational age ($P<0.001$; Fig. 1B), becoming scarce-to-absent in preterm infants older than 28 gw. Comparison between the five groups showed that $Sox2^+$ cells were fewer in 29–35 gw infants compared with 16–19, 20–22 and 26–28 gw ($P<0.001$, 0.026, 0.047, respectively). To determine whether $Sox2^+$ cells exhibited apical and basal processes, we double labeled the sections with Sox2 and vimentin antibodies. Vimentin was expressed on basal and apical processes of the radial glia surrounding the $Sox2^+$ nuclear labeling (Fig. 3A). Many $Sox2^+$ cells showed vimentin positive apical processes; however, the basal processes could not be traced deep into the white matter. Similarly, nestin was expressed on radial glial processes encircling the $Sox2^+$ nuclear labeling (Fig. 3B)

Similar to $Sox2^+$ cells, $Tbr2^+$ IPC were abundant in the SVZ of fetuses and premature infants (16–28 gw, Fig. 1 and 2). A pairwise comparison between the five groups of subjects showed a progressive decline in the number of $Tbr2^+$ cells with advancing gestational age ($P<0.001$ for three comparisons: 16–19 vs. 20–22 gw, 20–22 vs. 23–25 gw, and 23–25 vs. 29–35 gw; $P<0.03$ for 23–25 vs. 26–28 gw, Fig. 1B). Notably, $Tbr2^+$ cells were almost undetectable after 28 gw. A subset of neuronal progenitors co-expressed Sox2 and Tbr2, suggesting persistence of Sox2 antigen after the birth of $Tbr2^+$ IPC. These Sox2 and Tbr2 co-labeled cells of the VZ and SVZ reduced in density with increasing gestational age ($P<0.001$, Fig. 1C), becoming extinct after 28 gw.

NIH-PA Author Manuscript

NIH-PA Author Manuscript

NIH-PA Author Manuscript

The fetuses of less than 23 gw usually do not survive and thus, are considered non-viable (Seri and Evans, 2008). We, therefore, compared the density of radial glia and IPC between fetuses of less than 23 gw (16–22 gw, non-viable) and premature infants of 23 gw or more (23–28 gw, viable). To this end, we combined 2 subsets of fetuses (16–19 and 20–22 gw) and 2 subsets of preterm infants (23–25, 26–29 gw), and then compared these two groups. We found that the density of $Sox2^+$, $Tbr2^+$, and both Sox2/Tbr2 positive cells was significantly less in preterm infants compared to fetuses ($P<0.025$, 0.001, 0.001, respectively). Together these results indicate that neurogenesis slows down as gestational age advances toward the age of viability.

Radial glia and IPC were more numerous in the inner SVZ compared with the outer SVZ in fetuses. Conversely, in preterm infants, $Tbr2^+$ cells appeared to be more abundant in the outer SVZ than the inner SVZ. Therefore, we compared densities of $Sox2^+$ and $Tbr2^+$ cells between the outer SVZ and the inner SVZ (including VZ) in 2 subsets of preterm infants—23–25 and 26–28 gw. We found that $Tbr2^+$ cells exhibited a trend towards higher density in the outer SVZ, whereas $Sox2^+$ cells displayed a trend for larger number in the inner SVZ. However, the comparisons were not statistically significant (Data not shown). Together, the relative abundance of apical ($Sox2^+$) and basal ($Tbr2^+$) neuronal progenitors in the VZ and SVZ of premature infants of 23–28 gw and their disappearance after 28 weeks suggests that glutamatergic neurogenesis continues until 28 gw.

Proliferation of neuronal progenitors is reduced in preterm infants compared to fetuses

To evaluate proliferation of radial glia and IPC in the dorsal SVZ, forebrain sections triple labeled with $Sox2^+$, $Tbr2^+$ and Ki67 specific antibodies were evaluated (Fig. 2). A comparison between 16–19, 20–22, 23–25, 26–28, and 29–35 gw categories revealed that $Ki67^+$ neural cells were abundant in lower gestational age and markedly sparse in higher gestational age subjects ($P<0.001$ for all three: 16–19 vs. 20–22 gw, 16–19 vs. 23–25 gw, and 20–22 vs. 26–28 gw; $P<0.028$ for 23–25 than 29–35 gw). Accordingly, proliferating $Sox2^+$ and $Tbr2^+$ cells were more numerous in early gestational age compared to late gestational age in fetuses and premature infants (Fig. 2B, 2C). Indeed, proliferation of all three categories of progenitors--$Sox2^+$, $Tbr2^+$, and cells co-expressing $Sox2^+$ and $Tbr2^+$--decreased with the advance in gestational age ($P<0.001$ all). Consistent with these findings, proliferation of $Sox2^+$ and $Tbr2^+$ cells was significantly higher in fetuses relative to premature infants (16–22 vs. 23–28 gw: $P<0.001$ all).

To specifically evaluate the density of radial glial cells after M-phase of the cell cycle, we chose another marker, phosho-vimentin (p-vimentin), and double labeled the brain sections with p-vimentin and Sox2 antibodies (Fig. 3C). We found that p-$vimentin^+$ cells were abundant in the dorsal VZ and SVZ of fetuses (16–22 gw), relatively scarce in premature infants of 23–25 gw, and almost absent after 26 gw (data not shown). Together, proliferation of neural progenitors in VZ and SVZ sharply declines in preterm infants, being almost absent after 28 gw.

Intermediate progenitors absent, but radial glia abundant in the ganglionic eminence

In humans, $Tbr2^+$ IPC, which are primarily glutamatergic, originate in the SVZ of dorsal telencephalon, whereas interneurons derive from both the dorsal SVZ and the ganglionic eminence (Letinic et al., 2002; Rakic and Zecevic, 2003; Kowalczyk et al., 2009). Accordingly, $Tbr2^+$ cells were conspicuously absent in the ganglionic eminence. The distribution of $Tbr2^+$ cells exhibited a sharp demarcation between abundant $Tbr2^+$ cells in the dorsal (cortical) SVZ and a complete absence of $Tbr2^+$ cells in the ventrally located ganglionic eminence (Fig. 4A).

NIH-PA Author Manuscript

NIH-PA Author Manuscript

NIH-PA Author Manuscript

Radial glia, labeled by Sox2, were abundant in the ganglionic eminence of fetuses and premature infants; and they declined in density with advancing gestational age ($P<0.001$, Fig. 4B, 4C). Accordingly, a comparison between groups revealed that the number of $Sox2^+$ cells in the ganglionic eminence was significantly decreased in some of the higher gestational age categories relative to lower age groups ($P<0.001$ for 16–19 vs. 23–25 gw; $P=0.017$ for 20–22 vs. 29–35 gw; $P=0.013$ for 25–28 vs. 29–35 gw, Fig. 4B, 4E). However, the difference in the density of $Sox2^+$ cells between fetuses (16–22 gw) and premature infants (23–28 gw) was not statistically significant.

We next assessed proliferation in the radial glia of the ganglionic eminence. Similar to the dorsal SVZ, the number of cycling neural cells ($Ki67^+$ cells) and proliferation specific to $Sox2^+$ progenitors (co-labeled $Sox2^+$ and $Ki67^+$) diminished with advancing gestational age ($P<0.001$ both, Fig. 4D). Consequently, these two categories of proliferating cells were more abundant in fetuses relative to premature infants ($P<0.05$ both). Consistent with these findings, a further comparison between the five groups showed significantly higher proliferation rates for lower gestational age groups (Fig. 4D). Collectively, these results demonstrate that in the ganglionic eminence $Tbr2^+$ cells were conspicuously absent; and the total number of $Sox2^+$ progenitors as well as their proliferation was reduced with increasing gestational age.

Cycling radial glia are more abundant in the ganglionic eminence relative to the dorsal SVZ

Since radial glia reside in both the dorsal SVZ and ganglionic eminence (Zecevic et al., 2005; Fietz and Huttner, 2010), it is important to compare their densities and proliferation capacity between these two germinal zones. The densities of $Sox2^+$ cells both in the fetuses (16–22 gw) and premature infants (23–28 gw) were comparable between the ganglionic eminence and the cortical SVZ. In addition, the pairwise comparison of the five groups between the two brain regions showed no significant difference.

We next compared the density of cycling $Sox2^+$ cells between the two germinal regions. The number of all cycling neural cells and proliferating $Sox2^+$ cells were significantly more in the ganglionic eminence relative to the dorsal SVZ in fetuses ($P=0.02$, 0.007), but not in premature infants ($P=.09$, 0.4). Accordingly, all cycling cells ($Ki67^+$) and proliferating $Sox2^+$ (co-labeled for Sox2 and Ki67) cells in 16–19 gw subjects were more abundant in the ganglionic eminence compared to the dorsal SVZ ($P< 0.001$ both), but no difference was found for the comparison between other groups. Together, these data suggest that cycling radial glia are more abundant in the ganglionic eminence compared to the dorsal SVZ in fetuses (16–22 gw), but not in premature infants.

Doublecortin positive cells in the ganglionic eminence and dorsal SVZ

Doublecortin (DCX), a microtubule-associated protein, is expressed in migrating neuroblasts and is a marker of newly generated neurons (Meyer, 2007). Hence, we quantified DCX^+ cells in the dorsal SVZ and ganglionic eminence in 4 sets of brains: 16–22, 23–25, 26–28 and 29–35 gw (n=4 each group, total 16). The percentage of DCX^+ cells (ratio of DCX^+ and $sytox^+$) ranged 20–30% and was comparable between the four gestational groups both in dorsal SVZ and ganglioic eminence (Fig. 5A, 5B). Accordingly, the total number of DCX^+ cells did not change as a function of gestational age and was similar between the groups (Fig. 5C).

We next evaluated proliferation of DCX^+ cells. In the ganglionic eminence, the total number of proliferating DCX^+ cells (co-labeled for DCX^+ and $Ki67^+$) reduced as a function of gestational age. Accordingly, the density of the proliferating DCX^+ cells was higher in 23–

NIH-PA Author Manuscript

NIH-PA Author Manuscript

NIH-PA Author Manuscript

25 gw compared to 25–28 and 29–35 gw (P<0.03 and 0.02 respectively, Fig. 5D). Similar to the ganglionic eminence, the proliferating DCX^+ cells in the dorsal SVZ showed a trend toward decline with the advance in gestational age, but the comparisons were not statistically significant.

Overall, the densities of total and proliferating DCX^+ cells were higher in the ganglionic eminence compared with the dorsal SVZ (P= 0.02, 0.032). Pairwise comparison between the two brain regions for each age group showed that the DCX^+ cells and cycling DCX^+ cells (co-labeled for DCX and Ki67) were more abundant in the ganglionic eminence compared with the dorsal SVZ for 23–25 gw (P= 0.002 both), but not for other gestational ages.

Preterm birth suppresses neurogenesis and dimethyloxallyl glycine restores neurogenesis in rabbits

Hypoxia activates proliferation and differentiation of neuronal progenitors (Soothill et al., 1986; Panchision, 2009); and preterm birth results in withdrawal of physiological hypoxia existing *in utero*. We, therefore, asked whether preterm birth affects the density and proliferation of $Sox2^+$ radial glial and $Tbr2^+$ IPC in the VZ and SVZ. To this end, we compared abundance of $Sox2^+$ and $Tbr2^+$ cells and their proliferation in just born term pups (E32, <2h age) and 3 days old premature (E29) rabbit pups (corrected conceptional age of 32 d) using stereological protocol. Double labeling with Tbr2 and Ki67 antibodies showed that both the densities of total $Tbr2^+$ and cycling $Tbr2^+$ cells were higher in term pups compared to preterm pups in the dorsal VZ and SVZ (P=0.025, 0.013, respectively; Fig. 6A, 6B). We next examined the cycling and non-cycling $Sox2^+$ cells in the two sets of pups. In contrast to $Tbr2^+$ progenitors, the density of total and proliferating $Sox2^+$ cells in the dorsal SVZ was fewer in term pups compared to preterm pups (P<0.05 both, Fig. 6C, 6D). We then compared the density of $Sox2^+$ cells in the lateral ganglionic eminence between the two groups. Similar to the dorsal SVZ, $Sox2^+$ cells in the ganglionic eminence were significantly less in term pups compared to preterm pups (63,884 ± 8,840 vs. 103,258 ± 14,143. P<0.05), but not the cycling Sox2 cells (25,527 ± 4,848 vs. 33,022 ± 4,664). Together, preterm birth suppressed glutamatergic neurogenesis and expanded radial glia population.

Preterm pups were exposed to normal oxygen concentration of room air for 3 days, whereas term pups were in the hypoxic uterine environment and were in room air for <2 h. Hypoxia stabilizes and normoxia degrades hypoxia-inducible factor (HIF-1α)—the master regulator of oxygen homeostatsis (Harten et al., 2010). Dimethyloxallyl glycine (DMOG), a hypoxia mimetic, stabilizes and enhances HIF-1α activity by suppressing the enzyme propyl hydroxylase (Harten et al., 2010). Therefore, we hypothesized that HIF-1α activation by DMOG treatment would restore glutamatergic neurogenesis in preterm pups. To this end, we alternatively treated E29 pups with either DMOG (100mg/kg once daily for 3 days) or vehicle and compared the density of $Sox2^+$ and $Tbr2^+$ cells between the two groups using stereological protocol (Fig. 7A, 7C. We found that DMOG treatment significantly increased the density of total $Tbr2^+$ (P<0.05), but not the cycling $Tbr2^+$ cells in the dorsal SVZ (P=0.1, Fig. 7B). DMOG treatment also reduced the density of proliferating $Sox2^+$ cells in the dorsal SVZ (P=0.02), but not the total density of $Sox2^+$ cells (P=0.1, Fig. 7D). We speculate that DMOG treatment reduced proliferation and enhanced differentiation of radial glia into IPC in the dorsal SVZ, resulting in increased population of $Tbr2^+$ IPC. A comparison of $Sox2^+$ cells in the ganglionic eminence revealed that the DMOG treatment reduced the density of both total and cycling $Sox2^+$ cells in preterm pups compared to vehicle controls (P=0.047 and 0.007, respectively). Together, preterm birth suppressed glutamatergic neurogenesis, and treatment with DMOG promoted glutamatergic neurogenesis in preterm rabbit pups.

NIH-PA Author Manuscript

NIH-PA Author Manuscript

NIH-PA Author Manuscript

Term rabbit pups exhibit higher HIF-1α, EPO and VEGF levels compared to preterm pups

The term pups (just born) were relatively hypoxic compared to preterm pups; and DMOG treatment in preterm pups might activate HIF-1α and upregulate HIF-1α induced molecules (Harten et al. 2010). Therefore, we postulated that HIF-1α, VEGF, and EPO levels would be reduced in preterm pups and DMOG treatment would increase the expression of these molecules. To this end, we measured the levels of HIF-1α, VEGF, and EPO in term, untreated preterm, and DMOG-treated preterm pups. We found that EPO mRNA expression, assayed by qRT-PCR, was significantly lower in preterm pups compared to term pups and that DMOG treatment increased the levels in preterm pups ($P<0.05$ and 0.01 respectively, Fig. 8A). Accordingly, VEGF mRNA accumulation showed a trend towards decrease in preterm pups relative to term pups ($P=0.08$) and DMOG treatment significantly enhanced VEGF expression in preterm pups ($P<0.05$, Fig. 8A).

To determine the protein expression of VEGF and HIF-1α, we performed Western blot analyses. Consistent with mRNA expression, VEGF protein levels were significantly reduced in preterm pups and DMOG treatment increased the level ($P<0.01$ each, Fig. 8B). Similarly, HIF-1α protein expression was reduced in preterm pups and DMOG treatment resulted in a significant elevation in its level ($P<0.05$ and 0.01 respectively; Fig. 8B). Together, rabbit pups *in utero* exhibit high levels of HIF-1α, VEGF and EPO, preterm delivery and room air exposure reduces their expression, and treatment of preterm pups with hypoxia-mimetics elevates their expression.

Preterm birth elevates and DMOG treatment restores Pax6 and Neurogenin expression

Glutamatergic neurogenesis in the dorsal telencephalon is orchestrated under the influence of graded expression of transcription factors, including Pax6, Neurogenin (Ngn)1/2, Hes1/5, Emx1/2, and Insm1 (Bertrand et al., 2002; Harten et al. 2010). Of these, Pax6 is the key transcription factor that maintains neuronal precursors in 'predifferentiation' state and regulates Ngn1/2 (S. Bel-Vialar et al., 2007). Thus, we postulated that preterm pups would exhibit higher Pax6 and Ngn1/2 expression compared to term pups and that DMOG treatment might restore their levels. To this end, we compared mRNA expression of Pax6, Ngn1/2, Emx1/2, and Insem1 in term, untreated preterm and DMOG treated preterm pups. We found that expression of Pax6 and Ngn2 was significantly higher in preterm pups compared to term pups ($P=0.033$ and 0.027) and DMOG treatment showed a trend towards decrease in their levels ($P>0.1$ and 0.09, Fig. 9A). Ngn1 gene expression was also significantly elevated in preterm pups compared to term pups and DMOG treatment reduced the level ($P< 0.01$ ea, Fig. 9A). However, expression of Hes1/5, Emx1/2, and Insm1 were comparable between the three groups (Fig. 9B, data on Emx1/2 not shown).

Since Pax6 is a key transcription factor regulating neurogenesis (Harten et al. 2010) and was significantly higher in preterm pups compared to term pups, we measured Pax6 protein levels by Western blot analyses. Consistent with gene expression, Pax6 levels were significantly elevated in preterm pups compared to term pups and DMOG treatment significantly reduced Pax6 levels in preterm pups ($P<0.01$ each, Fig. 9C). Collectively, proneural genes including Pax6 and Ngn1/2 are elevated in preterm pups, which appear to expand $Sox2^+$ population and arrest the generation of $Tbr2^+$ IPC.

DISCUSSION

About 10% of infants are born premature worldwide and these infants are at high risk of neurodevelopmental disabilities, cognitive dysfunctions, and behavioral disorders. Since the prematurity rate is increasing and because the survival of these infants has markedly improved, the neurodevelopmental sequelae in preterm infants have emerged as a major

NIH-PA Author Manuscript

NIH-PA Author Manuscript

NIH-PA Author Manuscript

public health concern. Little is known about neurogenesis in the third trimester of pregnancy when preterm infants are born, and the impact of premature birth on neurogenesis is also elusive. In this study, we evaluated neurogenesis in human fetuses and premature infants of 16–35 gw, assessed the effect of preterm birth on neurogenesis in premature rabbit pups, and used DMOG, a HIF-1α activator, to restore neurogenesis in preterm rabbits. We found that significant neurogenesis continued in preterm infants until 28 gw. In addition, preterm birth suppressed glutamatergic neurogenesis, and HIF-1α activation restored neurogenesis in preterm rabbit pups.

The most novel finding of this study is that neurogenesis continued in the premature infants until 28 gw. We demonstrated that both cycling and non-cycling $Sox2^+$ radial glial cells as well as $Tbr2^+$ IPC were abundant in preterm infants of 23–28 gw, reduced in density with advancing gestational age, and disappeared by 29 gw. Our findings are consistent with the data that the total number of neural cells in the human brain increases from ~13×10^9 at 20 weeks of intrauterine life to 19–23×10^9 in the adult brain (Samuelsen et al., 2003), indicating persistence of neurogenesis beyond 20 gw. Persistence of neurogenesis in late pregnancy has enormous clinical significance; its suppression upon premature birth might contribute to the abnormal neuro-radiological and neuro-behavioral manifestations prevalent in preterm infants. A prominent reduction in gray matter volume of cerebral cortex on MRI evaluation, relatively small head circumference on clinical examination, and prevalence of neurodevelopmental disabilities on neurobehavioral assessment in premature neonates can be attributed to perinatal insults--hypoxia, ischemia, sepsis and necrotizing enterocolitis—adversely affecting the developmental neurogenesis (Inder et al., 2005; Dyet et al., 2006; Thompson et al., 2007). Worldwide rates of cognitive impairment in preterm infants increase with a decrease in gestational age (14–39% for 24 gw, 10–30% for 25 gw, 4–24% for 26 gw, and 11–18% for 29 gw; (Emsley et al., 1998; Stephens and Vohr, 2009). This inverse relationship between gestational age and the incidence of cognitive disability, inattention, hyperactivity, and abnormal motor outcomes in premature infants suggests that neurogenesis is suppressed in these infants secondary to preterm birth and perinatal insults (Vohr and Msall, 1997). Hence, persistence of neuronal turnover in the preterm infants of 23–28 gw underscores the need to minimize neonatal complications that might adversely affect neurogenesis.

Another key finding of this study is that preterm birth suppressed glutamatergic neurogenesis. This conclusion was based on a comparison between two groups of rabbit pups of equivalent postconceptional age--term pups (E32) of less than 2 h age and preterm pups (E29, premature by 10% gestation) of 72 h postnatal age. The term pups were in a relatively hypoxic environment *in utero*, whereas preterm pups were exposed to normal oxygen concentration of the room air for 3 days. A number of studies have shown that mild hypoxia (2.5–5% O_2) promotes stem cell proliferation (De Filippis and Delia). Importantly, culture experiments on neuronal stem cells derived from the ganglionic eminence have shown that the exposure to low oxygen concentration facilitates their differentiation from GABA-positive into glutamate-positive neurons (Horie et al., 2008). Consistent with these findings, we observed that preterm pups in room air for 3 days exhibited a reduced number of $Tbr2^+$ cells (precursor of glutamatergic neurons) in the dorsal SVZ compared with immediately born term pups. Glutamatergic excitatory neurons constitute 80%, whereas GABAergic inhibitory interneurons comprise 20% of the cortical neuronal population. A disproportion between the two types of neurons is associated with epilepsy, autism, neurodevelopmental disorders, and psychiatric diseases. Indeed, these disorders are more common in prematurely born infants compared to mature ones (Whitaker et al., 1997; Indredavik et al., 2010). Interestingly, preterm birth resulting in premature visual stimulation does not change the rate of synaptogenesis, but leads to distinct changes in size, type and

NIH-PA Author Manuscript

NIH-PA Author Manuscript

NIH-PA Author Manuscript

laminar distribution of synapses (Bourgeois et al., 1989). Together, premature birth results in multiple morphological and molecular changes in the cerebral cortex.

This study identified that the use of a hypoxia mimetic (DMOG) restored glutamatergic neurogenesis in preterm pups. Specifically, the use of DMOG in preterm pups expanded the population of $Tbr2^+$ IPC and reduced the density of $Sox2^+$ radial glial cells. DMOG is an ester of N-oxalylglycine that inhibits the enzyme prolyl-4 hydroxylase to stabilize HIF-1α under normal oxygen tension (Harten et al., 2010). HIF-1α key regulator of oxygen homeostasis, and induces transcription of a number of genes, including EPO, VEGF and glucose transporters (Semenza, 2007). Accordingly, we observed higher expression of HIF-1α, EPO and VEGF in DMOG treated preterm pups relative to untreated preterm controls. Importantly, both EPO and VEGF stimulate neurogenesis (Studer et al., 2000; Sun et al., 2003). HIF-1α also affects several signaling pathways that regulate neuronal progenitors. It modulates WNT/β-catenin signaling in the hypoxic neuronal progenitors by upregulating β-catenin and downstream effectors, LEF1 and TCF-1 (Mazumdar et al., 2010). In addition, HIF-1α interacts with Notch-1 intracellular domain and is recruited to Notch responsive promoters when Notch is activated (Gustafsson et al., 2005). We observed lower levels of Pax6 transcription factor in just-born term pups compared with preterm pups in room air. In disagreement with this finding, intermittent hypoxia results in elevated expression of Pax6 transcription factor in cell culture experiments (Ross et al. 2012). This inconsistency between the studies may be because the effects of external and internal cues on proneural genes and neurogenesis are context dependent (Bertrand et al., 2002). High Pax6 and Ngn2 in our preterm (relative to term) animals seemingly increases the density of $Sox2^+$ cells (Roybon et al., 2009); and activation of HIF-1α (by DMOG) in premature pups downregulates Pax6 to enhance $Tbr2^+$ and reduce $Sox2^+$ cells. Hence, pharmacologic compounds that activate HIF-1α may be useful in premature human infants to restore neurogenesis. However, to our knowledge, these agents have not yet entered clinical trials.

Premature birth results in withdrawal of physiological hypoxia existing *in utero*. However, it also deprives the preterm newborn of placental hormones and growth factors, as well as maternal nutrients and hormones, which might impact neurogenesis and brain growth (Zeltser and Leibel 2011). While the placenta is a site to selectively transport maternal nutrients, growth factors, and hormones, it is also a primary source of neurotropic factors such as 5-hydroxytryptamine that affect neuronal proliferation and axonal growth (Bonnin et al. 211). Additionally, an absence of natural birth may result in failed induction of mitochondrial uncoupling protein or other molecules that might exert significant effect on neurogenesis (Simon-Areces et al., 2012). The present study did not evaluate the effect of maternal, placental, or any other factors that can potentially affect neurogenesis in preterm infants.

A major strength of this study is the use of autopsy materials from human infants. It has become abundantly clear that the cortical expansion in human is not just quantitative; however, human cortex exhibits novel types of neurons and cytoarchitectonic areas that do not exist in rodents and rabbits (Bystron et al., 2008; Clowry et al., 2011). While human tissues are invaluable, the infants dying in neonatal intensive care units because of prematurity, respiratory failure, or clinical sepsis might be associated with clinical variables that affect neurogenesis. To limit the potential confounding variables, we included only preterm infants of short postnatal age (<5d) in the study and excluded infants with hypoxia-ischemia, culture proven sepsis, major congenital defects, chromosomal defects, meningitis, and intraventricular hemorrhage of grade 2–4. Nevertheless, hypoxia-ischemia and systemic inflammatory response in preterm infants might influence neurogenesis. In a mouse model, chronic perinatal hypoxia has enhanced cortical neurogenesis and has resulted in preferential generation of $Tbr1^+$ excitatory neurons as opposed to $parvalbumin^+$ and $calretinin^+$

NIH-PA Author Manuscript

NIH-PA Author Manuscript

NIH-PA Author Manuscript

inhibitory neurons (Fagel et al., 2006; Fagel et al., 2009). Hence, the presented data should be interpreted with caution. The present study used a rabbit model to determine the effect of prematurity on neurogenesis. The rabbit brain is gyrecephalic and they exhibit a brain growth spurt between E22 and P5 (Harel et al., 1972). In rabbits, brain increases in weight by 7 fold from birth through adulthood compared to four-fold increase in humans druing this period, suggesting relatively less maturation of the rabbit brain at birth relative to humans (Harel et al., 1972).

In conclusion, developmental neurogenesis in the cortical SVZ slows down with advancing gestational age, but continues in the preterm infants until 28 gw. In addition, preterm birth inhibits glutamatergic neurogenesis that can be reversed by HIF-1α stabilizing agents. Persistence of neurogenesis in preterm infants underscores a need to minimize the complications of prematurity that may adversely affect neuronal turnover during this period. Agents that stimulate hypoxia transduction pathways might constitute useful therapies for preterm infants to enhance neurogenesis, promote cortical growth and improve neurodevelopmental outcome.

Acknowledgments

Authors thank Joanne Abrahams for the assistance with images.

Source of funding: NIH/NINDS grant RO1 NS071263 (PB), Scientist development grant from American Heart Association (GV), Marshall Klaus grant of American Academy of Pediatrics (SM).

REFERENCES

Ballabh P, Xu H, Hu F, Braun A, Smith K, Rivera A, Lou N, Ungvari Z, Goldman SA, Csiszar A, Nedergaard M. Angiogenic inhibition reduces germinal matrix hemorrhage. Nat Med. 2007; 13:477–485. [PubMed: 17401377]

Bel-Vialar S, Medevielle F, Pituello F. The on/off of Pax6 controls the tempo of neuronal differentiation in the developing spinal cord. Dev Biol. 2007; 305:659–673. [PubMed: 17399698]

Bertrand N, Castro DS, Guillemot F. Proneural genes and the specification of neural cell types. Nat Rev Neurosci. 2002; 3:517–530. [PubMed: 12094208]

Bonnin A, Goeden N, Chen K, Wilson ML, King J, Shih JC, Blakely RD, Deneris ES, Levitt P. A transient placental source of serotonin for the fetal forebrain. Nature. 2011; 472:347–350. [PubMed: 21512572]

Bourgeois JP, Jastreboff PJ, Rakic P. Synaptogenesis in visual cortex of normal and preterm monkeys: evidence for intrinsic regulation of synaptic overproduction. Proc Natl Acad Sci U S A. 1989; 86:4297–4301. [PubMed: 2726773]

Bystron I, Blakemore C, Rakic P. Development of the human cerebral cortex: Boulder Committee revisited. Nat Rev Neurosci. 2008; 9:110–122. [PubMed: 18209730]

Clowry G, Molnar Z, Rakic P. Renewed focus on the developing human neocortex. J Anat. 2011; 217:276–288. [PubMed: 20979582]

De Filippis L, Delia D. Hypoxia in the regulation of neural stem cells. Cell Mol Life Sci. 2011; 68:2831–2844. [PubMed: 21584807]

de Kieviet JF, Zoetebier L, van Elburg RM, Vermeulen RJ, Oosterlaan J. Brain development of very preterm and very low-birthweight children in childhood and adolescence: a meta-analysis. Dev Med Child Neurol. 2012; 54:313–323. [PubMed: 22283622]

Dummula K, Vinukonda G, Xu H, Hu F, Zia MT, Braun A, Shi Q, Wolk J, Ballabh P. Development of integrins in the vasculature of germinal matrix, cerebral cortex, and white matter of fetuses and premature infants. J Neurosci Res. 2011; 88:1193–1204. [PubMed: 19960540]

Dyet LE, Kennea N, Counsell SJ, Maalouf EF, Ajayi-Obe M, Duggan PJ, Harrison M, Allsop JM, Hajnal J, Herlihy AH, Edwards B, Laroche S, Cowan FM, Rutherford MA, Edwards AD. Natural history of brain lesions in extremely preterm infants studied with serial magnetic resonance

NIH-PA Author Manuscript

NIH-PA Author Manuscript

NIH-PA Author Manuscript

imaging from birth and neurodevelopmental assessment. Pediatrics. 2006; 118:536–548. [PubMed: 16882805]

Emsley HC, Wardle SP, Sims DG, Chiswick ML, D'Souza SW. Increased survival and deteriorating developmental outcome in 23 to 25 week old gestation infants, 1990-4 compared with 1984-9. Arch Dis Child Fetal Neonatal Ed. 1998; 78:F99–F104. [PubMed: 9577278]

Fagel DM, Ganat Y, Cheng E, Silbereis J, Ohkubo Y, Ment LR, Vaccarino FM. Fgfr1 is required for cortical regeneration and repair after perinatal hypoxia. J Neurosci. 2009; 29:1202–1211. [PubMed: 19176828]

Fagel DM, Ganat Y, Silbereis J, Ebbitt T, Stewart W, Zhang H, Ment LR, Vaccarino FM. Cortical neurogenesis enhanced by chronic perinatal hypoxia. Exp Neurol. 2006; 199:77–91. [PubMed: 15916762]

Fietz SA, Huttner WB. Cortical progenitor expansion, self-renewal and neurogenesis-a polarized perspective. Curr Opin Neurobiol. 2010; 21:23–35. [PubMed: 21036598]

Gustafsson MV, Zheng X, Pereira T, Gradin K, Jin S, Lundkvist J, Ruas JL, Poellinger L, Lendahl U, Bondesson M. Hypoxia requires notch signaling to maintain the undifferentiated cell state. Dev Cell. 2005; 9:617–628. [PubMed: 16256737]

Hansen DV, Lui JH, Parker PR, Kriegstein AR. Neurogenic radial glia in the outer subventricular zone of human neocortex. Nature. 2010; 464:554–561. [PubMed: 20154730]

Harel S, Watanabe K, Linke I, Schain RJ. Growth and development of the rabbit brain. Biol Neonate. 1972; 21:381–399. [PubMed: 4657752]

Harten SK, Ashcroft M, Maxwell PH. Prolyl hydroxylase domain inhibitors: a route to HIF activation and neuroprotection. Antioxid Redox Signal. 2010; 12:459–480. [PubMed: 19737089]

Haubensak W, Attardo A, Denk W, Huttner WB. Neurons arise in the basal neuroepithelium of the early mammalian telencephalon: a major site of neurogenesis. Proc Natl Acad Sci U S A. 2004; 101:3196–3201. [PubMed: 14963232]

Horie N, Moriya T, Mitome M, Kitagawa N, Nagata I, Shinohara K. Lowered glucose suppressed the proliferation and increased the differentiation of murine neural stem cells in vitro. FEBS Lett. 2004; 571:237–242. [PubMed: 15280049]

Horie N, So K, Moriya T, Kitagawa N, Tsutsumi K, Nagata I, Shinohara K. Effects of oxygen concentration on the proliferation and differentiation of mouse neural stem cells in vitro. Cell Mol Neurobiol. 2008; 28:833–845. [PubMed: 18236013]

Inder TE, Warfield SK, Wang H, Huppi PS, Volpe JJ. Abnormal cerebral structure is present at term in premature infants. Pediatrics. 2005; 115:286–294. [PubMed: 15687434]

Indredavik MS, Vik T, Evensen KA, Skranes J, Taraldsen G, Brubakk AM. Perinatal risk and psychiatric outcome in adolescents born preterm with very low birth weight or term small for gestational age. J Dev Behav Pediatr. 2010; 31:286–294. [PubMed: 20431402]

Jakovcevski I, Mayer N, Zecevic N. Multiple origins of human neocortical interneurons are supported by distinct expression of transcription factors. Cereb Cortex. 2011; 21:1771–1782. [PubMed: 21139075]

Kowalczyk T, Pontious A, Englund C, Daza RA, Bedogni F, Hodge R, Attardo A, Bell C, Huttner WB, Hevner RF. Intermediate neuronal progenitors (basal progenitors) produce pyramidal-projection neurons for all layers of cerebral cortex. Cereb Cortex. 2009; 19:2439–2450. [PubMed: 19168665]

Letinic K, Zoncu R, Rakic P. Origin of GABAergic neurons in the human neocortex. Nature. 2002; 417:645–649. [PubMed: 12050665]

Mazumdar J, O'Brien WT, Johnson RS, LaManna JC, Chavez JC, Klein PS, Simon MC. O2 regulates stem cells through Wnt/beta-catenin signalling. Nat Cell Biol. 2010; 12:1007–1013. [PubMed: 20852629]

Meyer G. Genetic control of neuronal migrations in human cortical development. Adv Anat Embryol Cell Biol. 2007; 189:1–111. 1 p preceding 1. [PubMed: 17212070]

Noctor SC, Martinez-Cerdeno V, Ivic L, Kriegstein AR. Cortical neurons arise in symmetric and asymmetric division zones and migrate through specific phases. Nat Neurosci. 2004; 7:136–144. [PubMed: 14703572]

NIH-PA Author Manuscript NIH-PA Author Manuscript NIH-PA Author Manuscript

Panchision DM. The role of oxygen in regulating neural stem cells in development and disease. J Cell Physiol. 2009; 220:562–568. [PubMed: 19441077]

Rakic S, Zecevic N. Emerging complexity of layer I in human cerebral cortex. Cereb Cortex. 2003; 13:1072–1083. [PubMed: 12967924]

Ross HH, Sandhu MS, Cheung TF, Fitzpatrick GM, Sher WJ, Tiemeier AJ, Laywell ED, Fuller DD. In vivo intermittent hypoxia elicits enhanced expansion and neuronal differentiation in cultured neural progenitors. Exp Neurol. 2012; 235:238–245. [PubMed: 22366327]

Roybon L, Hjalt T, Stott S, Guillemot F, Li JY, Brundin P. Neurogenin2 directs granule neuroblast production and amplification while NeuroD1 specifies neuronal fate during hippocampal neurogenesis. PLoS One. 2009; 4:e4779. [PubMed: 19274100]

Samuelsen GB, Larsen KB, Bogdanovic N, Laursen H, Graem N, Larsen JF, Pakkenberg B. The changing number of cells in the human fetal forebrain and its subdivisions: a stereological analysis. Cereb Cortex. 2003; 13:115–122. [PubMed: 12507942]

Sanai N, Nguyen T, Ihrie RA, Mirzadeh Z, Tsai HH, Wong M, Gupta N, Berger MS, Huang E, Garcia-Verdugo JM, Rowitch DH, Alvarez-Buylla A. Corridors of migrating neurons in the human brain and their decline during infancy. Nature. 2011; 478:382–386. [PubMed: 21964341]

Semenza GL. Life with oxygen. Science. 2007; 318:62–64. [PubMed: 17916722]

Seri I, Evans J. Limits of viability: definition of the gray zone. J Perinatol. 2008; 28(Suppl 1):S4–S8. [PubMed: 18446176]

Simon-Areces J, Dietrich MO, Hermes G, Garcia-Segura LM, Arevalo MA, Horvath TL. UCP2 induced by natural birth regulates neuronal differentiation of the hippocampus and related adult behavior. PLoS One. 7:e42911. [PubMed: 22905184]

Simon-Areces J, Dietrich MO, Hermes G, Garcia-Segura LM, Arevalo MA, Horvath TL. UCP2 induced by natural birth regulates neuronal differentiation of the hippocampus and related adult behavior. PLoS One. 2012; 7:e42911. [PubMed: 22905184]

Soothill PW, Nicolaides KH, Rodeck CH, Gamsu H. Blood gases and acid-base status of the human second-trimester fetus. Obstet Gynecol. 1986; 68:173–176. [PubMed: 3090491]

Stephens BE, Vohr BR. Neurodevelopmental outcome of the premature infant. Pediatr Clin North Am. 2009; 56:631–646. Table of Contents. [PubMed: 19501696]

Studer L, Csete M, Lee SH, Kabbani N, Walikonis J, Wold B, McKay R. Enhanced proliferation, survival, and dopaminergic differentiation of CNS precursors in lowered oxygen. J Neurosci. 2000; 20:7377–7383. [PubMed: 11007896]

Sun Y, Jin K, Xie L, Childs J, Mao XO, Logvinova A, Greenberg DA. VEGF-induced neuroprotection, neurogenesis, and angiogenesis after focal cerebral ischemia. J Clin Invest. 2003; 111:1843–1851. [PubMed: 12813020]

Thompson DK, Warfield SK, Carlin JB, Pavlovic M, Wang HX, Bear M, Kean MJ, Doyle LW, Egan GF, Inder TE. Perinatal risk factors altering regional brain structure in the preterm infant. Brain. 2007; 130:667–677. [PubMed: 17008333]

Vasileiadis GT, Gelman N, Han VK, Williams LA, Mann R, Bureau Y, Thompson RT. Uncomplicated intraventricular hemorrhage is followed by reduced cortical volume at near-term age. Pediatrics. 2004; 114:e367–e372. [PubMed: 15342899]

Vohr BR, Msall ME. Neuropsychological and functional outcomes of very low birth weight infants. Semin Perinatol. 1997; 21:202–220. [PubMed: 9205976]

Wang C, Liu F, Liu YY, Zhao CH, You Y, Wang L, Zhang J, Wei B, Ma T, Zhang Q, Zhang Y, Chen R, Song H, Yang Z. Identification and characterization of neuroblasts in the subventricular zone and rostral migratory stream of the adult human brain. Cell Res. 2011; 21:1534–1550. [PubMed: 21577236]

Whitaker AH, Van Rossem R, Feldman JF, Schonfeld IS, Pinto-Martin JA, Tore C, Shaffer D, Paneth N. Psychiatric outcomes in low-birth-weight children at age 6 years: relation to neonatal cranial ultrasound abnormalities. Arch Gen Psychiatry. 1997; 54:847–856. [PubMed: 9294376]

Zecevic N, Chen Y, Filipovic R. Contributions of cortical subventricular zone to the development of the human cerebral cortex. J Comp Neurol. 2005; 491:109–122. [PubMed: 16127688]

Zeltser LM, Leibel RL. Roles of the placenta in fetal brain development. Proc Natl Acad Sci U S A. 2011; 108:15667–15668. [PubMed: 21890794]

Zheng X, Linke S, Dias JM, Gradin K, Wallis TP, Hamilton BR, Gustafsson M, Ruas JL, Wilkins S, Bilton RL, Brismar K, Whitelaw ML, Pereira T, Gorman JJ, Ericson J, Peet DJ, Lendahl U, Poellinger L. Interaction with factor inhibiting HIF-1 defines an additional mode of cross-coupling between the Notch and hypoxia signaling pathways. Proc Natl Acad Sci U S A. 2008; 105:3368–3373. [PubMed: 18299578]

NIH-PA Author Manuscript

NIH-PA Author Manuscript

NIH-PA Author Manuscript

NIH-PA Author Manuscript

NIH-PA Author Manuscript

NIH-PA Author Manuscript

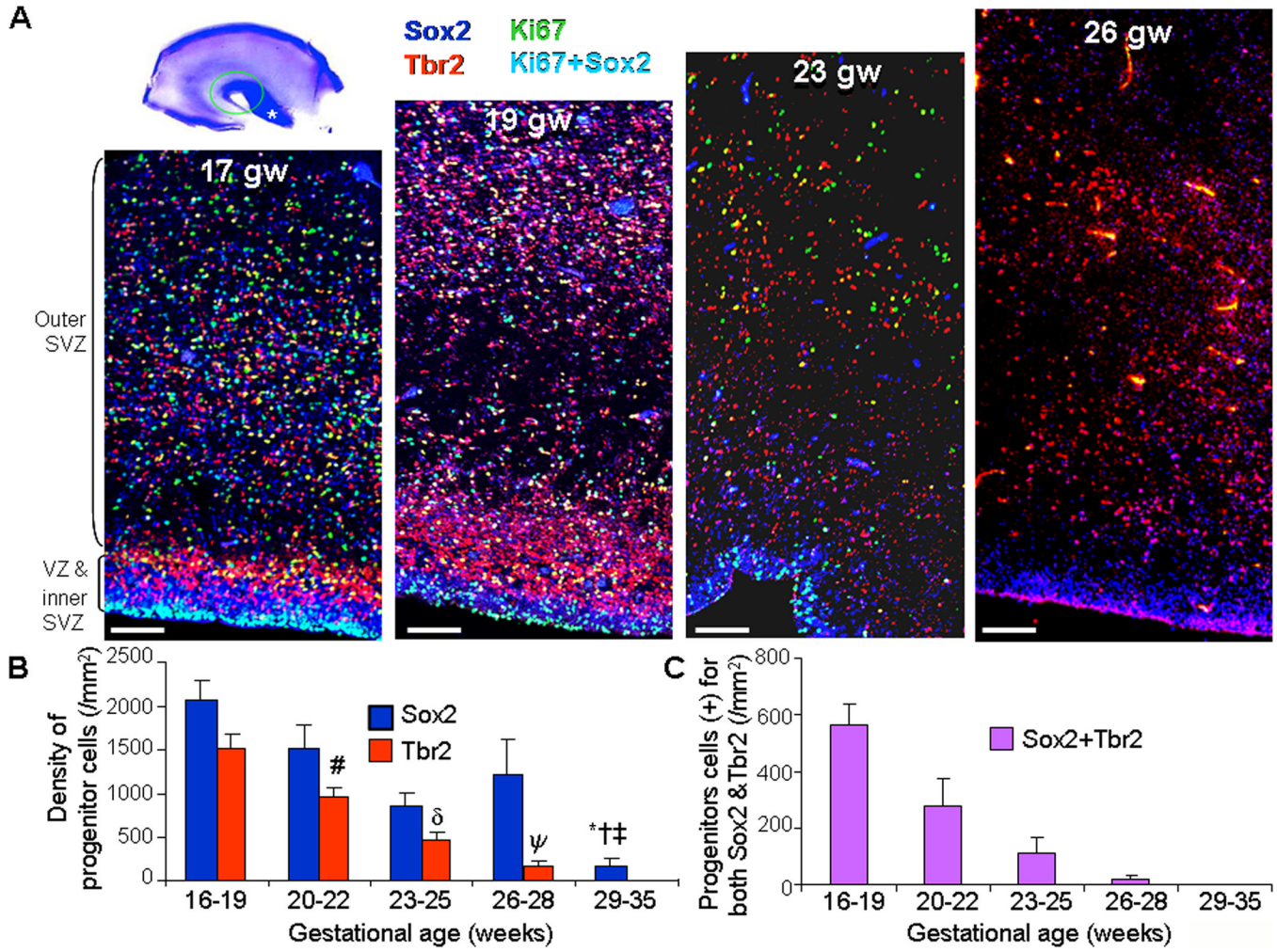

Fig. 1. Neurogenesis continues in dorsal SVZ until 28 gw

A. Representative immunofluorescence of cryosections from subjects of 17, 19, 23 and 26 gw, triple labeled with Sox2, Tbr2 and Ki67 antibodies. There was an abundance of $Sox2^+$ and $Tbr2^+$ neuronal progenitors in the VZ and SVZ that decrease in density with increasing gestational age. Cresyl violet stained coronal section from 17 gw forebrain (left top) shows dorsal cortical SVZ (white circle) and ganglionic eminence (asterisk); all images were acquired in dorsal SVZ. Scale bar, 100 μm. **B**. Densities of $Sox2^+$ and $Tbr2^+$ cells progressively reduce with advancing gestational age, becoming scarce after 28 gw. Bar charts are mean ± sem. * $P<0.001$, † $P=0.026$ and ‡ $P=0.047$ for the comparison of $Sox2^+$ cells between 29–35 gw vs. 16–19, 20–22 and 26–28 gw, respectively. # and δ indicate $P<0.001$ each, for the comparison of $Tbr2^+$ cells between 16–19 vs. 20–22 gw and 20–22 vs. 23–25 gw. ψ indicates $P<0.03$ for the comparison of $Tbr2^+$ cells between 23–25 vs. 26–28 gw; **C**. Bar charts are mean ± sem. Neuronal progenitors co-expressing Sox2 and Tbr2 significantly decline in density with increasing gestational age, disappearing by 28 gw.

NIH-PA Author Manuscript

NIH-PA Author Manuscript

NIH-PA Author Manuscript

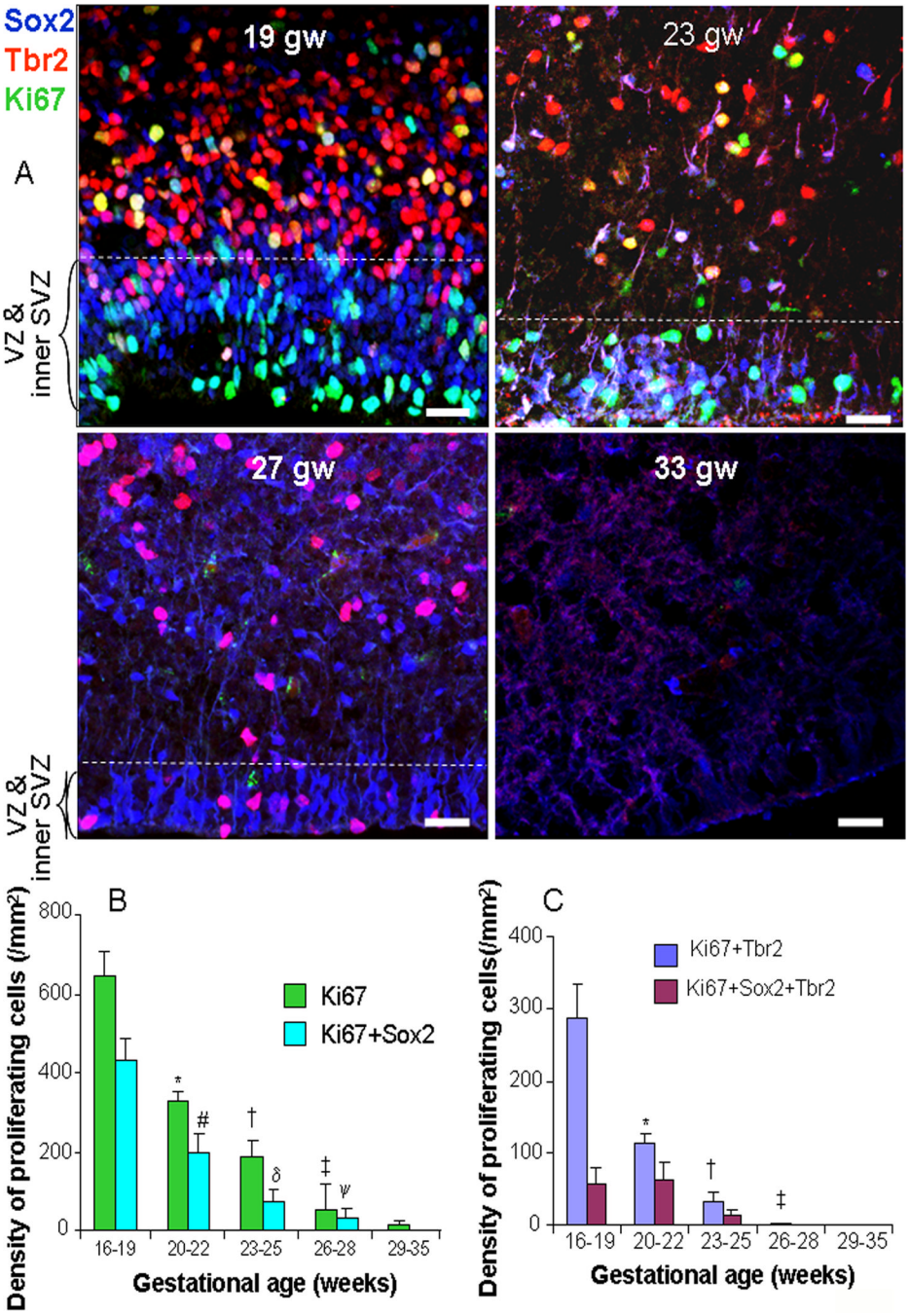

Fig. 2. Proliferation of apical and basal progenitors reduce with advancing gestation

A. Typical morphology of radial glia ($Sox2^+$) and IPC ($Tbr2^+$) in the VZ and SVZ of cryosections taken from 19, 23, 27 and 33 gw subjects triple labeled with Sox2, Tbr2, and Ki67 antibodies. The number of cycling and non-cycling $Sox2^+$ and $Tbr2^+$ cells reduces with increasing gestation, becoming completely absent by 33 gw. Scale bar, 25 μm. Dashed line indicates intersection of inner and outer SVZ. **B**. Densities of all proliferating cells and cycling $Sox2^+$ cells decreased with advancing gestational age. Bar charts are mean ± sem. *, † and ‡ indicate P<0.001 for the comparison of all proliferating cells ($Ki67^+$) for both 16–19 vs. 20–22 gw, 16–19 vs. 23–25 gw and 20–22 vs. 26–28 gw respectively. # and δ indicate

NIH-PA Author Manuscript

NIH-PA Author Manuscript

NIH-PA Author Manuscript

$P<0.001$ for $Sox2^+$ cells comparing 16–19 vs. 20–22 gw, 16–19 vs. 23–25 gw. ψ indicates $P=0.024$ for $Sox2^+$ cells comparing 20–22 vs. 26–28 gw. **C**. Densities of cycling cells labeled Tbr2 and co-labeled $Sox2^+$ and $Tbr2^+$ decreased with rising gestational age. Bar charts are mean ± sem. * and † indicate $P<0.001$ for the comparison of proliferating $Tbr2^+$ cells for both 16–19 vs. 20–22 gw and 16–19 vs. 23–25 gw. ‡ $P=0.008$, for the comparison of cycling $Tbr2^+$ cells at 20–22 vs. 26–28 gw.

NIH-PA Author Manuscript
NIH-PA Author Manuscript
NIH-PA Author Manuscript

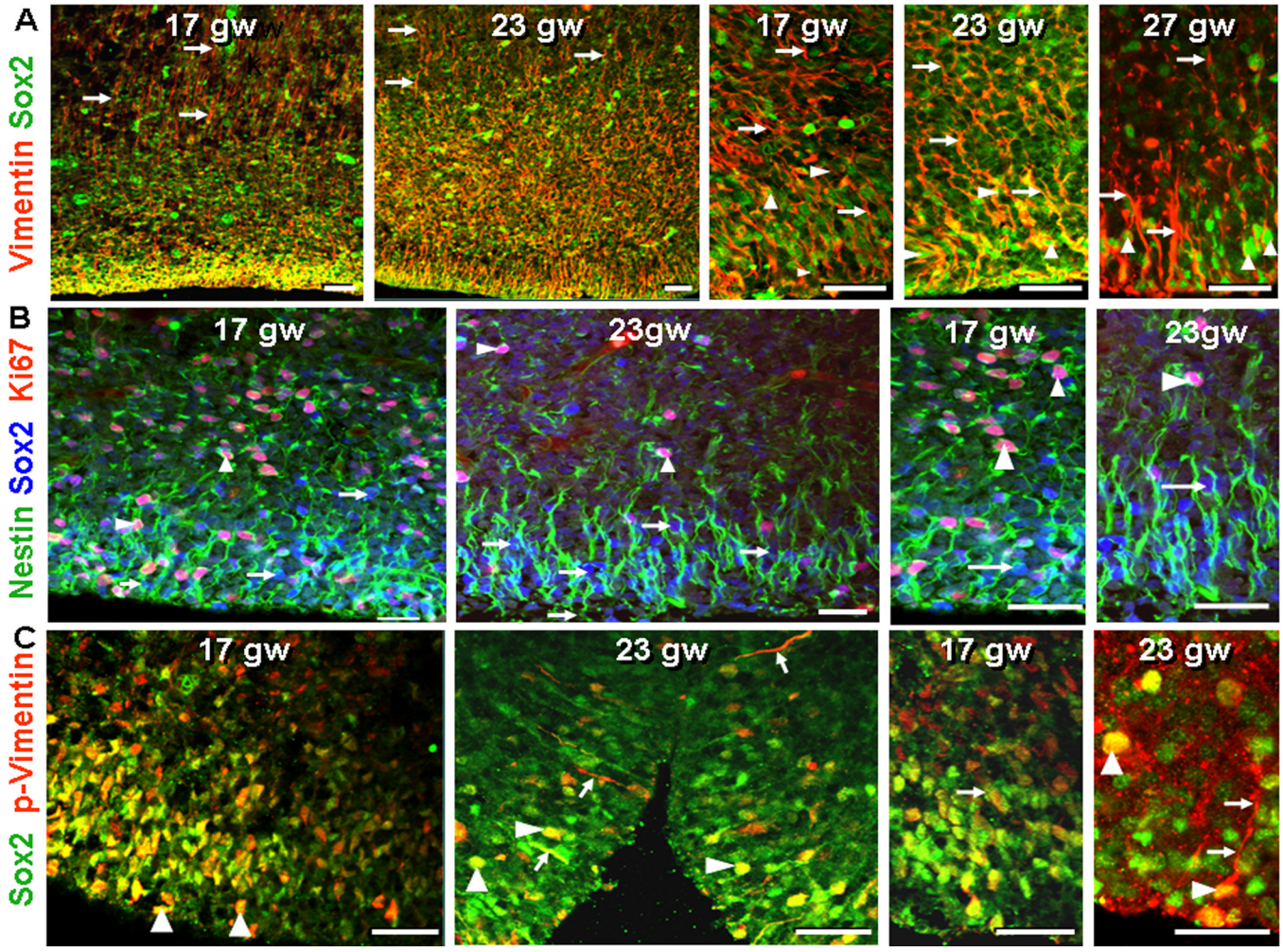

Fig. 3. Sox2$^+$ radial glial cells show apical and basal processes in fetuses and premature infants

A. Double immunolabeling at 17, 23 and 27 gw with Sox2 and vimentin antibodies. Note basal radial glial processes in outer SVZ (arrow) and predominance of Sox2$^+$ cells (arrowhead) in VZ and inner SVZ. Sox2$^+$ cells were embedded into vimentin. Scale bar, 25 μm. **B**. Triple immunolabeling of cryosections from 17 and 23 gw subjects with Sox2, nestin and Ki67 antibodies. Nestin positive radial glial processes surround the Sox2 (arrow) and Ki67 (arrowhead) positive nuclear signals. Scale bar, 25μm. **C**. In 17 and 23 gw subjects, double-labeling with Sox2 and p-vimentin antibodies shows co-localization of two immunoreactivities at several locations (arrowheads) indicating that the radial glial cells are in M-phase. Note the processes of p-vimentin$^+$ cells extending into SVZ (arrows). Scale bar, 25 μm.

NIH-PA Author Manuscript
NIH-PA Author Manuscript
NIH-PA Author Manuscript

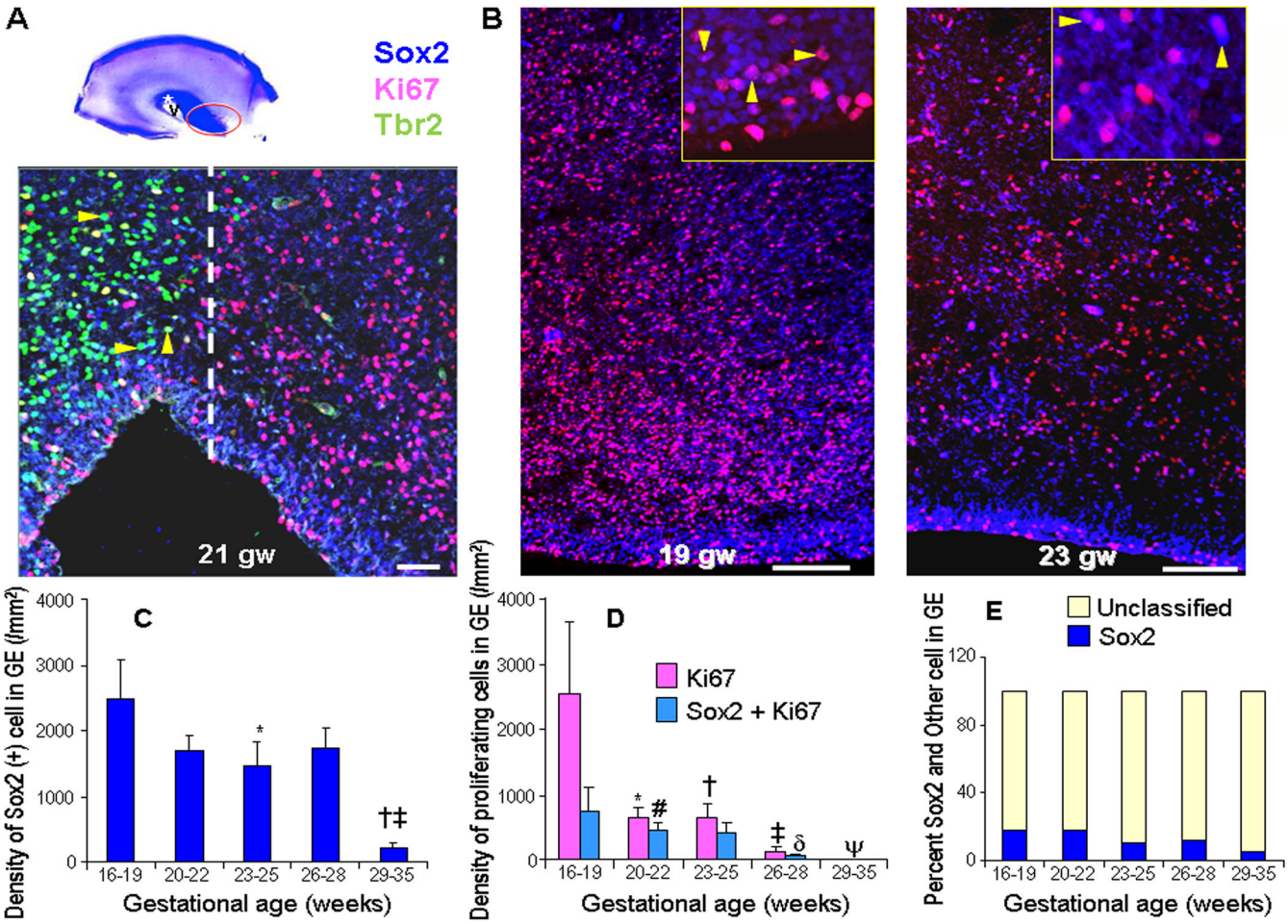

Fig. 4. Neurogenesis in ganglionic eminence continues until 28 gw

A. Representative immunofluorescence of cryosections from subjects of 21 gw, triple labeled with Sox2, Tbr2 and Ki67 antibodies. Note that $Tbr2^+$ cells (arrowheads) are absent in the ganglionic eminence; dashed line marks a sharp demarcation in the SVZ between dorsal (cortical) SVZ and ventrally located ganglionic eminence in respect to the distribution of $Tbr2^+$ cells. Scale bar, 50μm. Cresyl violet stained coronal section from 17 gw (left top) forebrain shows ganglionic eminence (red circle), dorsal cortical SVZ (asterisk) and lateral ventricle (V). Images in 'B" were acquired in the ganglionic eminence. **B**. Typical distribution of $Sox2^+$ and $Ki67^+$ cells in the ganglionic eminence of 19 and 23 gw infants. Note lesser density of $Sox2^+$ cells in 23 gw relative to 19 gw. Arrowhead indicates cycling $Sox2^+$ cells. Scale bar, 100μm. **C**. Note decreased density of $Sox2^+$ cells in lower age groups. Bar charts are mean ± sem. *P<0.001 for 16–19 vs. 23–25 gw; †P=0.017 for 20–22 vs. 29–35 gw; ‡P=0.013 for 26–28 vs. 29–35 gw. **D)** All cycling neural cells and proliferating $Sox2^+$ cells decreased in density with advancing gestational age. Bar charts are mean ± sem. For all cycling cells: *P<0.007 for 16–19 vs. 20–22 gw; † and ‡ P<0.01 for 16–19 vs. 23–25 and 26–28 gw respectively. For proliferating $Sox2^+$ cells: #, δ and ψ, P<0.001 for 16–19 gw vs 20–22, 26–28 and 29–35 gw. **E)** Proportional bar diagram showing reduction in the density of percent Sox^+ cells with advancing gestational age.

NIH-PA Author Manuscript
NIH-PA Author Manuscript
NIH-PA Author Manuscript

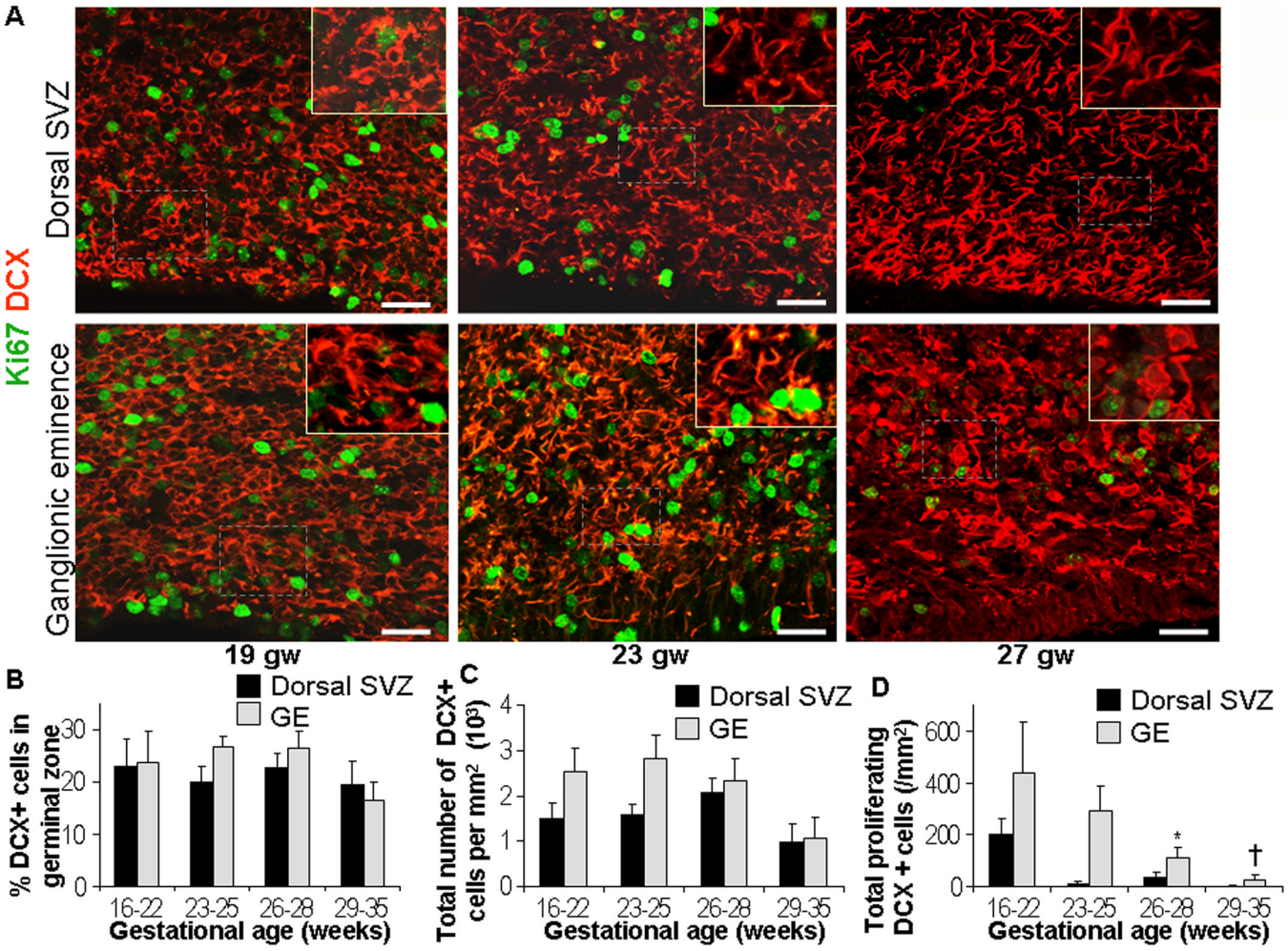

Fig. 5. DCX$^+$ cells are similar in density across gestational age categories in both the ganglionic eminence and dorsal SVZ

A. Representative immunofluorescence of cryosections from subjects of 19, 23 and 27 gw, double labeled with DCX and Ki67 antibodies. Note densities of DCX$^+$ cells are comparable between the 19, 23 and 27 gw subjects in both dorsal SVZ (upper panel) and ganglioic eminence (lower panel), whereas number of proliferating cells (Ki67$^{+)}$ is greatly reduced during the same period. Scale bar, 25μm. **B**. Note that percentages of DCX$^+$ cells (ratio of DCX$^+$ and sytox$^+$) are comparable across the gestational age categories in both dorsal SVZ and ganglionic eminence. Bar charts are mean ± sem. **C**. Total number of DCX$^+$ cells was comparable across gestational age categories in both the dorsal SVZ and ganglionic eminence. Bar charts are mean ± sem. **D**. Number of proliferating DCX$^+$ (DCX$^+$ and Ki67$^+$) cells significantly reduced as a function of gestational age in ganglionic eminence. However, in the dorsal SVZ, cycling DCX$^+$ cells showed a trend towards reduction in density with advancing gestation, which was not significant. Bar charts are mean ± sem. In ganglionic eminence for proliferating cells DCX$^+$ cells: * P=0.03 for 23–25 vs. 25–28 gw; † P= 0.02 for 23–25 vs. 29–35 gw.

NIH-PA Author Manuscript
NIH-PA Author Manuscript
NIH-PA Author Manuscript

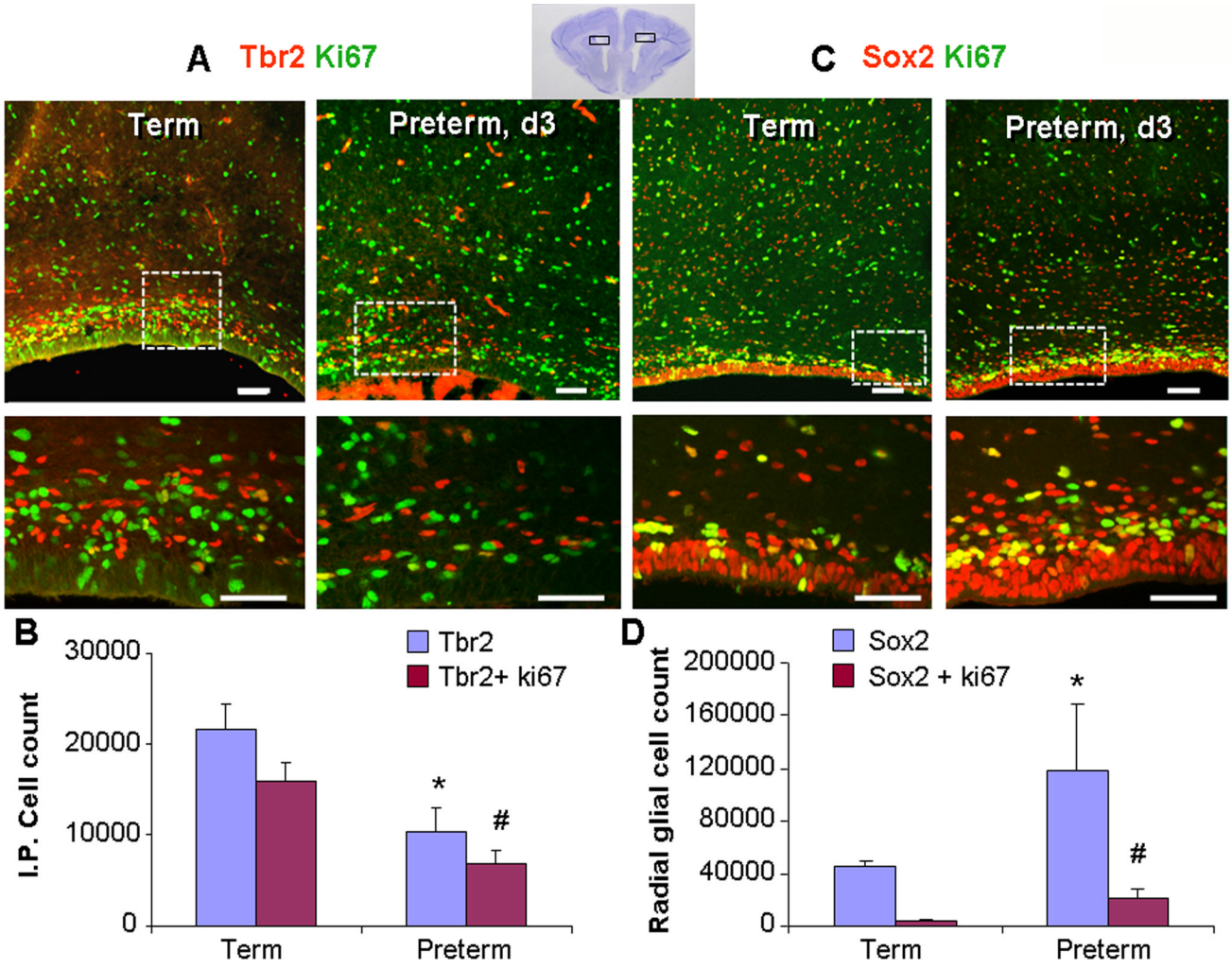

Fig. 6. Preterm birth in rabbits suppressed Tbr2$^+$ IPC and increased Sox2$^+$ radial glia cells

A. Representative immunofluorescence of the dorsal SVZ from 3 day old preterm pups and just born term pups double labeled with Tbr2 and Ki67 antibodies. Lower panel is higher magnification. Note the higher density of both proliferating and non-proliferating Tbr2$^+$ cells in term pups compared to preterm ones. Scale bar, 25μm. Cresyl violet stained coronal section from the forebrain of E29 rabbit pup (right top) shows dorsal cortical SVZ (box). **B**. The total number of Tbr2$^+$ and cycling Tbr2$^+$ cells were higher in term pups compared to preterm pups in dorsal VZ and SVZ. Bar charts are mean ± sem (n=5 each group). *P<0.02 and # P=0.01 for the comparison between preterm and term pups. **C**. Cryosections from 3 day old preterm pups and immediately born term pups were double labeled with Sox2 and Ki67 antibodies. Low (Upper panel) and high (lower panel) magnification of the dorsal SVZ. Total and proliferating Sox2$^+$ cells are less abundant in term pups compared to preterm ones. Scale bar, 25μm. **D**. Data are mean ± sem (n=5 each group). The total and proliferating Sox2$^+$ cells were fewer in term pups compared to preterm pups. * and # P <0.05 for the comparison between preterm and term pups.

NIH-PA Author Manuscript
NIH-PA Author Manuscript
NIH-PA Author Manuscript

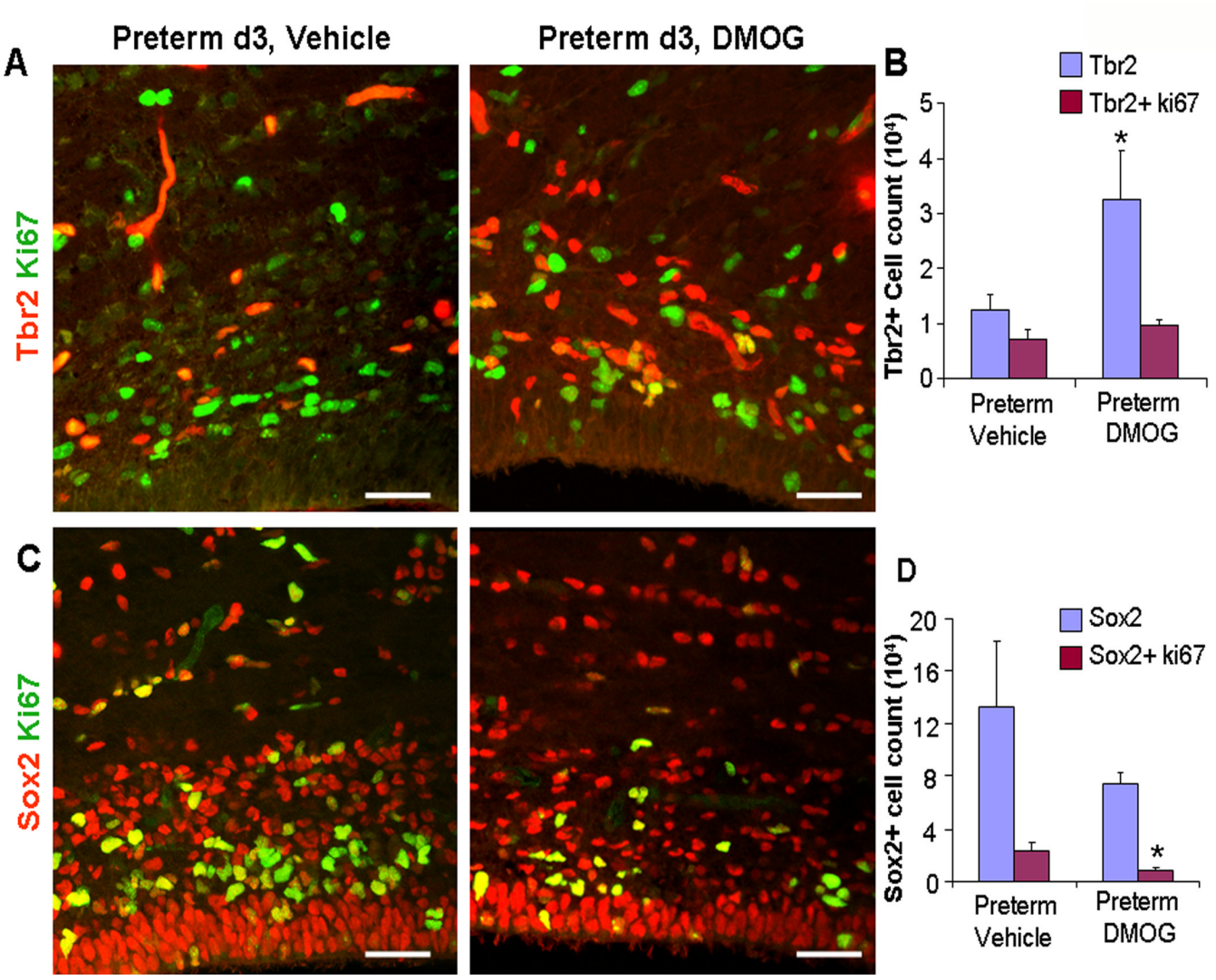

Fig. 7. DMOG treatment reversed glutamergic neurogenesis in preterm pups

A and C. Representative immunofluorescence of cryosections of dorsal VZ/SVZ from 3 day old preterm pups treated either with DMOG or vehicle. Sections were double labeled with Tbr2 and Ki67 (A) or Sox2 and Ki67 (C) antibodies. Note higher density of $Tbr2^+$ cells and lower density of $Sox2^+$ in DMOG-treated pups compared with vehicle controls. Scale bar, 25μm. **B**. Quantification of total and cycling $Tbr2^+$ cells in DMOG- and vehicle-treated preterm pups. Bar charts are mean ± sem (n=5 each group). *P <0.05 for the comparison between DMOG and vehicle treated preterm pups. **D**. The proliferating $Sox2^+$ cells were fewer in DMOG treated pups compared to vehicle controls. Data are mean ± sem (n=5 each group). *P <0.05 for the comparison between DMOG and vehicle treated preterm pups.

NIH-PA Author Manuscript
NIH-PA Author Manuscript
NIH-PA Author Manuscript

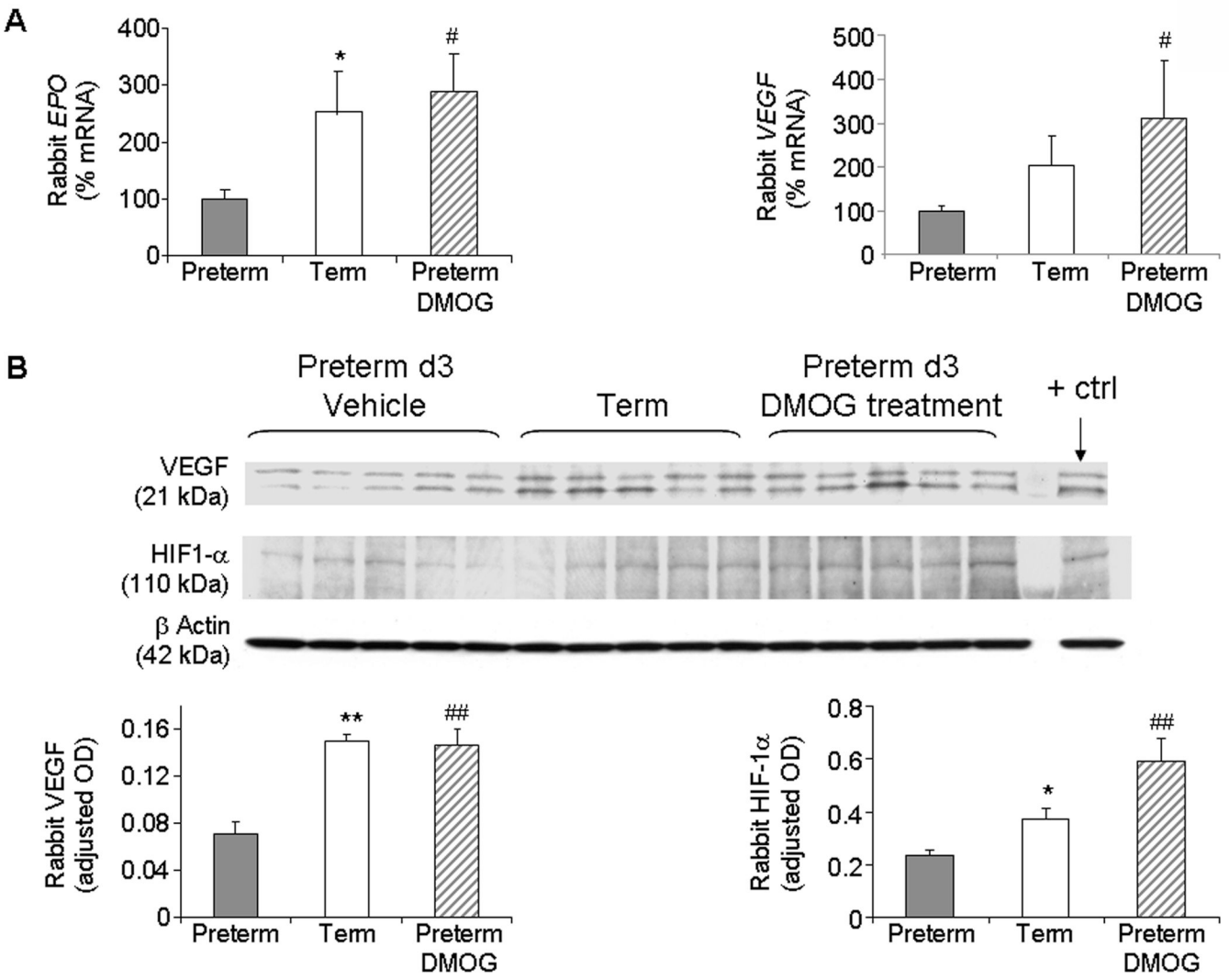

Fig. 8. Reduced HIF-1α, EPO and VEGF in preterm vs. term pups, and DMOG elevates them

A. Note EPO mRNA expression was reduced in preterm pups compared to term pups. VEGF mRNA accumulation showed a trend towards decrease in preterm pups relative to term pups. DMOG treatment elevated the levels of both EPO and VEGF. Data are mean ± sem. (n=5 each group). **B**. Representative Western blot analyses for VEGF and HIF-1α for term, untreated preterm, and DMOG-treated preterm pups. VEGF and HIF1α protein levels were significantly reduced in preterm infants than term pups and DMOG treatment increased the levels. Data are mean ± sem. (n=5 each group). Values are normalized to β actin levels. *P <0.05, **P<0.01 for the comparison between preterm and term pups. #P<0.05 and ## P<0.01 for the comparison between untreated and DMOG treated preterm pups.

NIH-PA Author Manuscript
NIH-PA Author Manuscript
NIH-PA Author Manuscript

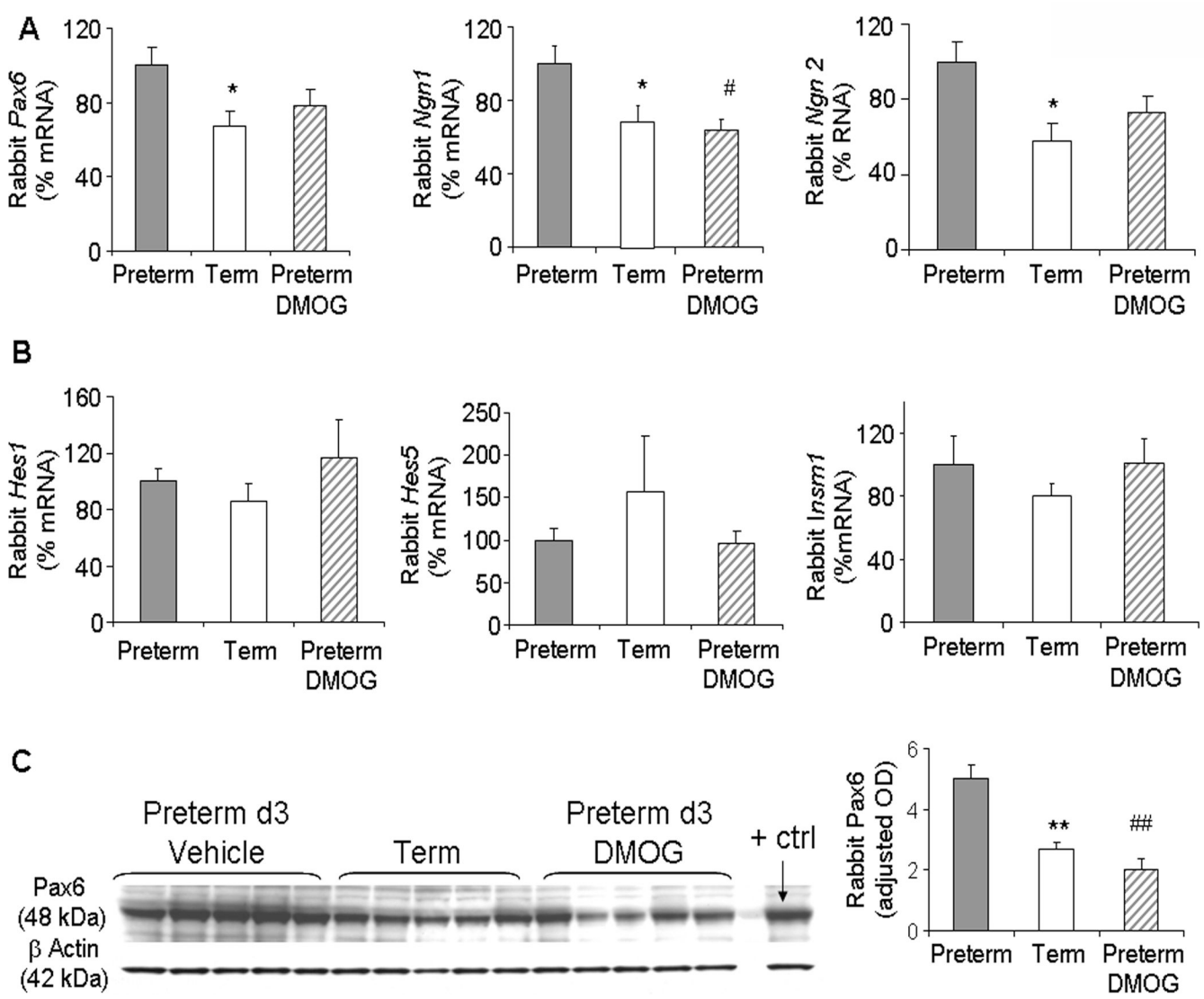

Fig. 9. Preterm birth elevates levels of Pax6 and neurogenin genes, and DMOG treament restores them

A. Data are mean ± sem. (n=5 each group). Note that Pax6 and Ngn 2 expression were significantly elevated in preterm pups compared with term pups. DMOG treatment in preterm pups showed a trend towards decrease relative to untreated preterm pups for both Pax6 and Ngn2. Ngn1 gene expression was also significantly higher in preterm pups relative to term pups and DMOG treament reduced the level. **B**. Hes1/5, Emx1/2, and Insm1 were similar between the three groups as indicated. **C**. Representative Western blot analyses for Pax6 for term, untreated preterm, and DMOG treated preterm pups. Data are mean ± sem. (n=5 each group). Values are normalized to β-actin levels. Pax6 levels were higher in preterm pups compared to term pups and DMOG treatment signfiicantly reduced Pax6 levels. *P <0.05. **P<0.01 for the comparison between preterm and term pups. #P<0.05 and ## P<0.01 for the comparison between untreated and DMOG treated preterm pups.

NIH-PA Author Manuscript
NIH-PA Author Manuscript
NIH-PA Author Manuscript

Table 1

Characteristics of human fetuses and premature infants studied

Case	Gestational age (weeks)	Weight (9)	Sex	clinical diagnosis and cause of death
1	16	--	Male	Cervical incompetence
2	17	--	Male	Undetermined
3	17	--	Female	Placental abruption
4	19	--	Male	Undetermined
5	19	240	Female	Cervical incompetence
6	20	360	Female	Multiple pregnancy
7	20	320	Male	Preterm labor
8	21	410	Female	Preterm labor
9	21	460	Male	Preterm labor
10	22	510	Male	Preterm labor
11	23	400	Female	Immaturity and respiratory failure
12	23	630	Male	Immaturity and respiratory failure
13	24	390	Male	Immaturity and respiratory failure
14	25	740	Male	Clinical sepsis
15	25	730	Female	Metabolic acidosis, cardioresp. failure
16	26	920	Female	Clinical sepsis and shock
17	27	550	Female twin	Respiratory failure
18	27	925	Male	Respiratory failure
19	27	480	Male	Clinical sepsis
20	28	900	Male	Respiratory failure
21	31	3390	Male	Hydrops Fetalis
22	32	992	Male	Necrotizing enterocolites
23	33	3380	Male	Non-immune hydrops
24	33	2305g	Female	Diaphragmatic hernia
25	35	2900	Female	Oligohydramnios, hypoplastic lung